Spring 5-31-2015

Design, construction and characterization OFA magnetic augmented rotation system (MARS) based wind turbine

Da Li
New Jersey Institute of Technology

Copyright Warning & Restrictions

The copyright law of the United States (Title 17, United States Code) governs the making of photocopies or other reproductions of copyrighted material.

Under certain conditions specified in the law, libraries and archives are authorized to furnish a photocopy or other reproduction. One of these specified conditions is that the photocopy or reproduction is not to be "used for any purpose other than private study, scholarship, or research." If a, user makes a request for, or later uses, a photocopy or reproduction for purposes in excess of "fair use" that user may be liable for copyright infringement,

This institution reserves the right to refuse to accept a copying order if, in its judgment, fulfillment of the order would involve violation of copyright law.

Please Note: The author retains the copyright while the New Jersey Institute of Technology reserves the right to distribute this thesis or dissertation

Printing note: If you do not wish to print this page, then select "Pages from: first page # to: last page #" on the print dialog screen

ABSTRACT

DESIGN, CONSTRUCTION AND CHARACTERIZATION OF A MAGNETIC AUGMENTED ROTATION SYSTEM (MARS) BASED WIND TURBINE

by

Da Li

Magnetic Augmented Rotation System (MARS) works by magnetic field coupling, to transfer torque from the driver to the rotor without contact. This characteristic has significant applications to the wind turbine but research in combination of MARS and wind turbine has not been done in the literature. In this thesis, a small-scale wind turbine is designed, built and characterized in a prototype wind tunnel. The test results are analyzed and computer-aided software simulation is used as an auxiliary method to understand the mechanism of MARS. The power coefficient of this new wind turbine is estimated to be about 40%. The “gear ratio” is proportional to the magnetic poles. The magnetic coupling transfers torque well.

DESIGN, CONSTRUCTION AND CHARACTERIZATION OF A MAGNETIC AUGMENTED ROTATION SYSTEM (MARS) BASED WIND TURBINE

by
Da Li

A Thesis
Submitted to the Faculty of
New Jersey Institute of Technology
in Partial Fulfillment of the Requirements for the Degree of
Master of Science in Materials Science and Engineering

Interdisciplinary Program in Materials Science and Engineering

May 2015

APPROVAL PAGE

DESIGN, CONSTRUCTION AND CHARACTERIZATION OF A MAGNETIC AUGMENTED ROTATION SYSTEM (MARS) BASED WIND TURBINE

Da Li

Dr. Nuggehalli M. Ravindra, Thesis Advisor — Date
Director of Materials Science and Engineering Program, NJIT

Dr. Siva P.V. Nadimpalli, Committee Member — Date
Assistant Professor, Department of Mechanical and Industrial Engineering, NJIT

Dr. Michael Jaffe, Committee Member — Date
Research Professor, Department of Biomedical Engineering, NJIT

Mr. Peter Kaufman, Committee Member — Date
President and Chief Technical Officer, Public Service Solutions Inc.

BIOGRAPHICAL SKETCH

Author: Da Li

Degree: Master of Science

Date: May 2015

Undergraduate and Graduate Education:

- Master of Science in Materials Science and Engineering,
  New Jersey Institute of Technology, Newark, NJ, 2015

- Bachelor of Science in Materials Chemistry,
  East China University of Science and Technology,
  Shanghai, China, 2012

Major: Materials Science and Engineering

< To Baoguo Li and Xinli Wang, my beloved parents >
< Special gratitude to Ms. Meng Zhu, my first, unique and cherished girlfriend >
< I LOVE YOU >

ACKNOWLEDGMENTS

The graduate stage towards my Master's degree will be completed. Honestly, I would say if it were not for those who guided and supported me along the journey, I would not have the courage and strength to complete the degree. The unforgettable two years' experience is great treasure for my future. I would sincerely express my gratitude to the following people with whom my life becomes more splendid.

First, I would like to thank Professor N.M. Ravindra, my Thesis Advisor. His continuous advice towards my study, offering timely and effective solutions to my puzzles, encouragement and love expressed in his every word and behavior made me feel proud and confident in my graduate studies, no matter how tough the difficulties.

Next, I want to render sincere appreciation to my thesis committee members: Dr. Siva P.V. Nadimpalli, Dr. Michael Jaffe and Mr. Peter Kaufman. They offered timely help and penetrating suggestions for the improvement of my thesis.

Last but not least, I express my gratitude to teachers, colleagues, peers and friends at NJIT who gave me support and understanding.

TABLE OF CONTENTS

TABLE OF CONTENTS
(continued)

Chapter **Page**

TABLE OF CONTENTS
(continued)

Chapter **Page**

LIST OF TABLES

LIST OF FIGURES

LIST OF FIGURES
(Continued)

CHAPTER 1

INTRODUCTION

Magnetic Augmented Rotation System (MARS) works by magnetic coupling to transfer torque from the driver to the rotor without contact. This feature has significant applications in wind turbines but research in combination of MARS and wind turbine is seldom seen. The analysis and understanding of the mechanism of MARS and its actual performance in small-scale wind turbine are needed for further investigation.

In Chapter 1, a brief introduction to the thesis is presented. In Chapter 2, the fundamentals of magnetism are described. In Chapter 3, the principles and optimization of MARS will be explained. In Chapter 4, a small-scale wind turbine is designed, built and characterized in a prototype wind tunnel. A MARS prototype is built and its efficiency is measured. In Chapter 5, the test results are analyzed and computer-aided software simulation is used as an auxiliary method to understand the mechanism of MARS. The power coefficient of the new wind turbine, based on MARS, is estimated to be 44.5%. As a conclusion in Chapter 6, the “gear ratio” of MARS is proportional to the magnetic poles and the magnetic coupling transfers torque well.

CHAPTER 2

FUNDAMENTALS OF MAGNETIC MATERIALS

2.1 Fundamental Definition of Magnetism

2.1.1 Discovery of Magnetism

Magnetism is a physical phenomenon that cannot be seen, felt or touched. The interaction between magnetic materials and magnetic field is the proof of the existence of magnetism and a way to investigate it. Natural magnets have been found by humans for thousands of years. The south pointing spoon in China is one of the early rudimentary applications. As early as 83 A.D. people carved the south pointing spoon out of loadstones and put it on a plate where it can rotate freely and finally stop and align itself parallel to the magnetic field of the earth [1]. Early European explorers including Columbus utilized magnetic compass for navigation throughout their voyage. The discovery of the American continent is closely linked to the utilization of the magnetic compass [2].

Though these early findings have led to the establishment of contemporary magnetism, the comprehensive understanding of magnetism did not emerge as a science until the 17th century. It is William Gilbert who first realized that the earth is a giant magnet and contains a center of iron. He published these findings in his book “De Magnete” in 1600 [3]. The Danish physicist, Hans Christian Oersted, observed in his experiments that electric currents passing through a carrying wire would deflect a

compass needle and he concluded that this deflection was due to the magnetic field generated around the wire by the electric current [1]. Since then, scientists have been greatly interested in the magnetic field and have put much effort in investigating the relationship between the electric field and magnetic field.

2.1.2 Magnetic Field

Magnetic field is intangible but has realistic impact in the form of electric currents and magnetic materials. It is the magnetic effect of electric currents and magnetic materials. There are two separate vector fields: H field and B field. H field is the field of magnetic field strength and B field is the field of the flux density. In vacuum, the two fields have the same direction and the magnitude of the B field (with the unit Tesla, T) is proportional to the magnetic field strength H (with the unit of Amperes per meter, A/m), as is shown in the following equation:

$$B = \mu H \tag{2.1}$$

where μ is the magnetic permeability of a material.

Magnetic fields can be illustrated as magnetic field lines. In Figure 2.1, a scrap of iron, around a magnet, is seen to align along the direction of the magnetic field. Outside magnets, magnetic lines scatter from the North Pole and converge at the South Pole. But, inside the magnets, the magnetic field points to the opposite direction, from the South Pole to the North Pole. The magnetic field is a vector field, with both

direction and magnitude. Tracing a topographic path, a field line is used as a visualization tool to describe the locus of the field. The tangent line to the path at a certain point is considered to be parallel to the vector field at that point. The density of the lines, which is the number of field lines in unit area, shows the magnitude of the field vector.

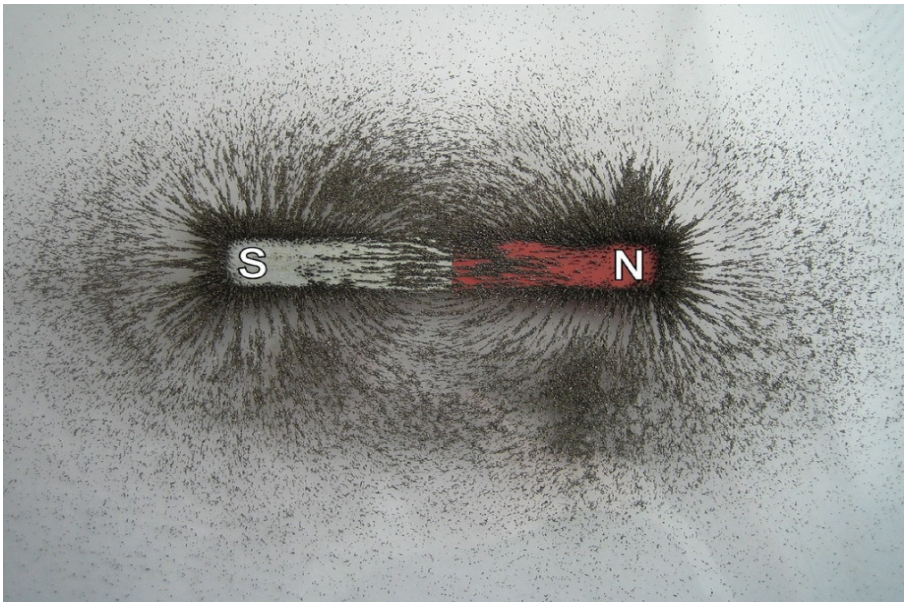

Figure 2.1 Magnetic field distribution around a bar magnet, visualized by scrap of iron.
Source: http://ask.newclasses.org/Detail_21160.aspx.

The magnitude of the magnetic fields can vary over a wide range. For example, common permanent magnets and electromagnets produce magnetic field of several Teslas. The strongest magnetic field is seen in magnetars that can reach up to 10^{11} Teslas [4].

2.1.3 Magnetic Dipoles and Magnetic Moment

A magnetic dipole is the limit of either of a closed loop of electric current or a pair of poles when the dimensions of the source are closely near zero with unchanged magnetic moment. A tiny dip needle can be considered as a dipole, with a “south pole” and a “north pole.” The dip needle can interact with the Earth’s magnetic field to direct North and South, since the Earth’s South Magnetic Pole is in the vicinity of geological North Pole so that it attracts the North Pole of a compass. The magnetic field around any magnetic source looks increasingly like the field of a magnetic dipole as the distance from the source increases.

The magnetic dipole can be analog to electric dipole, but unlike the electric dipole with positive and negative electrical charged particles, no magnetic monopole has been observed so far. The only discovery has been that the North and South Poles of a magnet cannot be separated from each other [5]. Scientists have been trying to find magnetic monopole for decades, although the existence of magnetic monopole has been predicted by some theoretical physicists such as Paul Dirac in the 20th century [6]. If the magnetic monopole is discovered someday, it will open a new door to the world of magnetism.

The magnetic moment of a magnet is a vector that shows the magnitude and direction of the torque that will be exerted in an external magnetic field. The direction of the magnetic moment points from the South Pole to North Pole of the magnet. The magnetic field generated by the magnet is proportional to its magnetic moment.

Rigidly speaking, the magnetic moment normally means the magnetic dipole moment since it is the first term in the multipole expansion, when the distance between the magnetic dipole is increasing, the first term becomes dominant of a general magnetic field [7]. The relationship is expressed as the following:

$$\tau = m \times B \tag{2.2}$$

where, $\boldsymbol{\tau}$ is the torque applied on the dipole, B is the external magnetic field and m is the magnetic moment. The torque τ on a small magnet is proportional both to the applied magnetic field and to the magnetic moment m of the magnet. The magnetic moment has the unit of *J/T*.

Magnetic moments may have two origins: microscopic electric currents resulting from the motion of electrons in atoms, or the spin of the electrons or the nuclei. The Bohr Magneton (μ_B) describes the magnetic dipole moment of an orbiting electron caused by either orbital or spin angular momentum. It is defined as:

$$\mu_B = \frac{e\hbar}{2m_e} = 9.27 \times 10^{-27} J/T \tag{2.3}$$

2.1.4 Magnetization

Magnetization, or the so called magnetic polarization is the vector field that shows the density of permanent or induced magnetic dipole moments in a magnetic material. Magnetic moment is responsible for magnetization. Magnetization is analog to

electric polarization. It describes both the way a material responds to the applied magnetic field and the way the materials changes the field. Net magnetization is due to the response of a material to external magnetic fields, and along with some unbalanced, inherent magnetic dipole moments. Magnetization is not usually uniformly distributed inside the material and depends on different locations. Magnetization is used to calculate the forces between the magnets and the applied magnetic field. It is defined as the quantity of magnetic moment per unit volume and is represented by vector M. Given magnetization, in B-field, the relationship between the B-field and H-field should be:

$$B = \mu_0(H + M) \tag{2.4}$$

2.1.5 Magnetic Energy

Magnetic energy is defined as the work of magnetic torque on re-alignment of the magnetic dipole moment m, and is equal to:

$$E_{p,m} = -mB \tag{2.5}$$

Energy will be stored when the current is passing through an inductor. The energy stored in the inductor, with inductance L, is equal to:

$$E_{p,m} = \frac{1}{2}LI^2 \tag{2.6}$$

Additionally, energy can be stored in a magnetic field. When the magnetic field is annihilated, the stored energy will be recycled and reused. In a medium with permeability μ and containing magnetic field B, the energy per unit volume, u, is equal to:

$$u = \frac{B^2}{2\mu} \tag{2.7}$$

2.1.6 Different Types of Magnetism in Materials

Diamagnetism appears in every material and is the property of a material which causes a repulsive effect to an externally applied magnetic field by creating an opposite magnetic field. An external magnetic field alters the orbital velocity of electrons around their nuclei, thus changing the magnetic dipole moment in the direction opposing the external field. Diamagnets usually have relative permeability less than 1. It is generally a weak effect in most materials, except for superconductors. Superconductors repel magnetic fields and are strongly diamagnetic. Using extremely strong superconducting magnets, diamagnetic objects such as pieces of lead can levitate.

Paramagnetic materials have positive magnetic susceptibility. Only a small fraction of spins will be oriented by the applied field so that it is also a weak effect and requires sensitive instrument to measure. This small fraction is proportional to the field strength, indicating the linear dependence of change in the magnetic dipole

moments. Magnetization of paramagnets will decrease to zero when the applied magnetic field is removed since thermal motion will cause the magnetic dipoles to be randomly oriented.

Ferromagnetism is the property of some permanent magnets and is detectable without the external field. Among all types of magnetism, the ferromagnetism (including ferrimagnetism) is the strongest one [8]. It can be felt in daily life because the forces created by ferromagnetism are strong and apparent to find, for example, the attraction between a magnet and a ferromagnetic material. It is a significant mechanism used in today's technology and industry and it is also the basis of many electrical and magnetic devices such electromagnets, electric generators, transformers etc.

Unlike ferromagnets, intrinsic magnetic moments of neighboring valence electrons tend to align in opposite direction in an antiferromagnet so that the entire system shows antiferromagnetism. Antiferromagnets have no net magnetic moment so that they cannot produce magnetic field. Antiferromagnetism is often seen at low temperatures and is less observed at room temperature. In changing temperatures, antiferromagnets can exhibit diamagnetic and ferromagnetic properties.

Ferrimagnets can also retain magnetization without an external field. Neighboring pairs of election spins inside ferrimagnets align in opposite directions. Since there is a distinct structure in ferrimagnets that more magnetic moment from the electrons align in one direction, these two properties can coexist in ferrimagnets. Most

ferrites are ferromagnetic, including the first discovered magnetic substance, magnetite.

When ferrimagnets are extremely small, such as to the extent of nanoscale, they will behave as single magnetic spins which are subject to Brownian motion. In this state, magnetization can randomly flip direction under the influence of temperature; so the magnetization is about zero, like paramagnetism, but its magnetic susceptibility is much larger than that in paramagnetism. So this feature is called superparamagnetism.

2.2 Important Laws of Electromagnetism

2.2.1 Coulomb's Law

Coulomb's law has made a great contribution to the understanding of electromagnetism. It is stated that the force between the two particle charges is directly proportional to the scalar multiplication of magnitude of the two charges and inversely proportional to the square of their distance. The force is along the straight line passing through the two particles. The direction of the force depends on the sign of the charges. If they have same sign, the force is repulsive, while it is attractive when they have different polarities [9].

$$F = k_e \frac{q_1 q_2}{r^2} \tag{2.8}$$

$$k_e = \frac{1}{4\pi\varepsilon_0} = 9 \times 10^9 Nm^2 C^{-2} \tag{2.9}$$

where F is the electrostatic force between the two particles with charges q_1 and q_2, respectively and r is their distance. k_e is Coulomb's constant.

2.2.2 Biot-Savart Law

Biot-Savart Law describes the magnetic field generated by steady electric current, a continual flow of charges which is constant in time and the charge neither accumulates nor depletes at any point, At a certain point P, the magnetic field that is generated by steady current I is expressed in Equations 2.10 and 2.11.

$$dB = \frac{\mu_0}{4\pi}\int_L \frac{Idl\sin\theta}{r^2} \tag{2.10}$$

$$B(r) = \frac{\mu_0}{4\pi}\int_L \frac{Idl\times r'}{r^2} \tag{2.11}$$

where I is the current, dl is the infinitesimal length of the conductor carrying electric current I, B is the generated magnetic field generated by Idl and r' is the unit vector from current element Idl to the point P. The law shows that the magnetic field at point P generated by the current element Idl is proportional to the magnitude of current element Idl and the sinusoidal value of the angle between Idl and r'. It is inversely proportional to the distance between the position P and the electric current element Idl.

2.2 3 Faraday's Law of Induction

The induced electromotive force (EMF) in any closed circuit is equal to the negative of the time of rate of change of the magnetic flux encompassed by the circuit, which is known as the Faraday's Law of Induction. In mathematical form, it is shown as:

$$E = -\frac{d\Phi}{dt} \tag{2.12}$$

where E is the electromotive force, Φ is the magnetic flux. The negative sign comes from Lenz's Law, meaning the induced current direction is always opposed to the change of flux. Faraday's Law of Induction is the basis of today's power generators.

2.2.4 Lorentz Force Law

In electromagnetism, the Lorentz force is the combination of electric and magnetic force on a point charge due to electromagnetic fields. If a particle of charge q moves with instantaneous velocity v in the presence of an external electric field E and a magnetic field B, then it will experience a force.

$$F = q(E + v \times B) \tag{2.13}$$

The term qE is the electric force part, while the term $qv \times B$ is the magnetic force part. When a current-carrying wire is placed in a magnetic field, every moving

charge will be exerted on Lorentz Force which could be integrated to a macroscopic force called Ampere Force.

$$\mathrm{F} = \mathrm{I} \int dl \times B = BIl \sin\theta \tag{2.14}$$

where B is the magnetic field, I is the current, l is the length of the current carrying wire, and θ is the angle between B and I. Ampere Force is the basis of today's electric motor.

2.2.5 Maxwell's Equations

Published by James Clerk Maxwell in the 19th century, Maxwell's equations are a series of partial differential equations describing how the electric and magnetic fields are produced and exchanged by each other and by charges and currents. Microscopic set and macroscopic set are the two variants of Maxwell's equations. The former one considers total charge and total current, with increasing universal applicability but reducing the calculation feasibility. The latter one ignores the complicated atomic-level details, and describes large-scale behavior by creating two auxiliary fields. However, the use of parameters is essential to characterize the electromagnetic properties of materials.

In Table 2.1, Maxwell's Equations are presented in two forms. The four equations in the left column is the integral form and the right column is the differential form. From top to bottom, in the table, the first row represents Gauss's

Law. The second row is Gauss's Law for Magnetism. Maxwell-Faraday Equation and Maxwell-Ampere Equation account for the third and last row.

Gauss's Law states that the net electric flux through any closed surface is equal to $1/\varepsilon_0$ times the net electric charge enclosed within that closed surface [10]. It can be derived from Coulomb's Law and vice versa.

Gauss's Law for Magnetism states that the magnetic field B has divergence equal to zero, demonstrating that the magnetic monopole does not exist [11]. With Maxwell's corrections, Faraday's Law of Induction becomes more general. It represents a time-varying magnetic field that is always accompanied by a spatially-varying, non-conservative electric field, and vice versa.

With Maxwell's extensions of displacement current, the Maxwell-Ampere Equation treats all charges on the same footing, regardless of whether they are bound or free charges; this breaks the limit of the original Ampere's Circuital Law.

Maxwell's Equations are the fundamental laws of electromagnetism. They are the foundation for electrodynamics. Maxwell's Equations unify the electric field and magnetic field, and predict that light is a kind of electromagnetic wave and expands the cognitive ability of humans to the physical world.

Table 2.1 Maxwell's Equations in Integral Form (Left Column) and Differential Form (Right Column)

$\oiint_{\partial\Omega} \mathbf{E} \cdot \mathrm{d}\mathbf{S} = \frac{1}{\varepsilon_0} \iiint_{\Omega} \rho \, \mathrm{d}V$	$\nabla \cdot \mathbf{E} = \frac{\rho}{\varepsilon_0}$
$\oiint_{\partial\Omega} \mathbf{B} \cdot \mathrm{d}\mathbf{S} = 0$	$\nabla \cdot \mathbf{B} = 0$
$\oint_{\partial\Sigma} \mathbf{E} \cdot \mathrm{d}\boldsymbol{\ell} = -\frac{d}{dt} \iint_{\Sigma} \mathbf{B} \cdot \mathrm{d}\mathbf{S}$	$\nabla \times \mathbf{E} = -\frac{\partial \mathbf{B}}{\partial t}$
$\oint_{\partial\Sigma} \mathbf{B} \cdot \mathrm{d}\boldsymbol{\ell} = \mu_0 \iint_{\Sigma} \mathbf{J} \cdot \mathrm{d}\mathbf{S} + \mu_0\varepsilon_0 \frac{d}{dt} \iint_{\Sigma} \mathbf{E} \cdot \mathrm{d}\mathbf{S}$	$\nabla \times \mathbf{B} = \mu_0 \left(\mathbf{J} + \varepsilon_0 \frac{\partial \mathbf{E}}{\partial t} \right)$

Source: http://en.wikipedia.org/wiki/Maxwell%27s_equations.

2.3 Magnetic Properties

2.3.1 Magnetic Permeability

Magnetic permeability is used to describe the ability of a material to form a magnetic field within itself and it is the degree of magnetization in response to the external magnetic field. It is defined by the following equation:

$$\mu = \frac{B}{H} \tag{2.15}$$

where μ is the magnetic permeability, with the SI unit of Henry per meter(Hm^{-1}) or Newtons per Ampere(NA^{-2}). Permeability is the inductance per unit length. In general, permeability is not a constant. It can change with the position in the medium, the frequency of the external magnetic field, humidity, temperature, and other parameters. It may also change with the external magnetic field.

Vacuum permeability, μ_0, is an ideal, physical constant that describes the value of the magnetic permeability in free space, which is equal to $4\pi\times10^{-7}$ N/A^2. It is an important constant and one of the three components defining free space through Maxwell's Equations. Relative permeability, μ_r, is the ratio of absolute permeability of a certain medium μ to μ_0, as shown in the following equation:

$$\mu_r = \frac{\mu}{\mu_0} \tag{2.16}$$

2.3.2 Magnetic Susceptibility

In electromagnetism, the magnetic susceptibility χ is a dimensionless proportionality constant that indicates the degree of magnetization of a material in response to an applied magnetic field. In Equations 2.17 and Equation 2.18, they are expressed as:

$$\chi = \mu_r - 1 \tag{2.17}$$

$$M = \chi H \tag{2.18}$$

Generally, the magnetization of a material refers to the sum of magnetic dipole moments per unit volume so that χ_m is also called the volumetric susceptibility. If ρ is the mass density of a material, the susceptibility per unit mass of a material is χ/ρ. Similarly, susceptibility per mole of a material with molar mass M is (χM/ρ).

Magnetic susceptibility is a significant parameter to identify the type of magnetism in magnetic materials. If χ is positive, a material exhibiting paramagnetism

and the magnetic field in the material will be enhanced by induced magnetization. On the contrary, when χ is negative, the material shows diamagnetism and the magnetic field in the material will be weakened. Ferromagnetic materials usually have high magnetic susceptibility.

2.3.3 Curie Temperature

Curie temperature, T_c, is a certain critical point in ferromagnetic materials. At the critical temperature, a material's intrinsic magnetic moments will change direction. When the temperature is above T_c, the ferrimagnets will lose all their magnetism because the intense thermal motion leads to the random and disorder configuration of magnetic dipoles so that the magnetic moments are not in uniform alignment anymore, though they still exhibit paramagnetism. Above this temperature, the material can no longer maintain its spontaneous magnetization so that its ability to be magnetized or attracted to a magnet disappears.

The Curie–Weiss law describes the magnetic susceptibility χ of ferrimagnets in the paramagnetic region above the Curie point:

$$\chi = \frac{C}{T - T_c} \tag{2.19}$$

where C is a material-specific Curie constant, T is absolute temperature in Kelvin, and T_c is the Curie temperature in Kelvin. The law shows that χ becomes infinite at the susceptibility at $T = T_c$. Higher temperatures will weaken magnets since

spontaneous magnetism only exists below T_c. Cooling and heat dissipation is very important in the working condition of magnetic components.

2.4 Magnetic Materials and Applications

Magnets always refer to materials being magnetized that would retain their own persistent magnetic field without applied external field. There are a few materials that can achieve this, and they are typically called permanent magnets. Ferromagnets or ferrimagnets, such as iron, cobalt and nickle are strongly attracted to a magnet. Some alloys of rare earth metals and natural materials such as lodestones form permanent magnets.

Magnetic materials can be classified into two groups by the difficulty of demagnetization: magnetically soft and hard magnets. Permanent magnets are considered as hard magnets with higher coercivity and remanence that are difficult to demagnetize unless a certain magnetic field is applied and the threshold value depends on the coercivity. Soft magnets can be magnetized but will lose magnetization while hard magnets tend to remain magnetized for a period of time. Common soft magnets are silicon steel, nickel steel and ferrites. They have small remanence and small coercivity; thus they are appropriate choices for devices working in alternating magnetic fields such as transformers and electric motors. Solenoids usually have iron core inside them that are made of soft magnets.

Electromagnets are a type of magnets in which the magnetic field is generated by electric current. The magnetic field will disappear when the current is removed. A magnetic core made of soft magnets will be wound by closely spaced turns of wire to concentrate the magnetic flux and make a strong magnet. Compared to permanent magnets, the magnetic field in electromagnets can be easily controlled and altered by adjusting the current passing through. But to retain the field, continuous electric current must be supplied. Electromagnets can be used in many devices such as motors, generators, relays, Magnetic resonance Imaging (MRI) machines etc. They can also be employed to move heavy iron-containing objects such as steel [12].

Diamagnetic substances such as carbon, copper, water and plastic are weakly repelled by a magnet. The permeability of diamagnetic materials is less than the magnetic constant. Paramagnetic substances such as platinum, aluminum and oxygen exhibit weaker attraction by several orders of magnitude than ferromagnets. An interesting finding is that ferrofluids usually do not retain magnetization in the absence of an externally applied field and thus are often classified as paramagnets or superparamagnets rather than ferromagnets [13].

Magnetic materials are widely used in various applications. Magnetic tapes, audio cassettes, hard disks can be used to store information and data. Cards and Automated Teller Machines (ATMs) have magnetic strips that encode information associated with bank accounts. Speakers and microphones have built-in permanent

magnets and current-carrying coils to convert electric energy into mechanical energy to amplify the sound.

Electric motors combine electromagnets and permanent magnets to convert electric energy into mechanical energy. Electric generators have the same structure but convert mechanical energy into electricity by moving a conductor in a magnetic field. Faraday's Laws of Induction play an important role in these devices.

Magnetic resonance imaging is used in hospitals to identify problems in human bodies without the need for a surgery. Nuclear magnetic resonance is used to characterize compounds in chemistry.

In engineering, magnets can pick up either tiny objects that are hard to hold in hand such as nails or heavy items such as scrap iron or steel. Some screwdrivers are equipped with magnets that can be used to hold tiny screws. In industry, magnets can separate magnetic materials from non-magnetic materials. The charging port of MacBook is an important design that avoids damage to the laptop when being tripped over by charging wire. Charging wire and the port are attached to each other by magnets. When someone is tripped by the wire, the two components will be disconnected to avoid the laptop from falling down to the ground.

Maglev is a new form of transportation which levitates in air by magnetic repulsion and is driven by electromagnetic force. It achieves very high speeds than other ground transportation vehicles due to the reduced friction.

CHAPTER 3

MAGNETIC AUGMENTED ROTATION SYSTEM (MARS)

In this chapter, a Magnetically Augmented Rotation System (MARS), based on US Patent 6356000 B1, will be introduced. MARS aims at improving the efficiency of the drive wheel and the prime mover by using magnetic coupling. MARS can be applied to various devices and some of the implications will be presented in this Chapter.

3.1 Rotation and Power Transmission

In two-dimensional scale, rotation is a circular movement of an object around a fixed point. Rotation axis is a virtual line that is usually defined in three-dimensional rotation of an object where the object rotates around this line. There are two types of rotation: spin and orbital revolution. One case is, if the axis passes through the body's center of mass, the body is said to rotate upon its own axis, or spin. A rotation about an external point, e.g. the Moon about the Earth, is called a revolution or orbital revolution, typically when it is produced by gravity.

Power generation, transmission and distribution are perpetual hot issues in the world. Hydraulic mills may be one of the most primitive machines that are used in agriculture. Wheels are pushed and start to rotate when impacted by falling liquid (water) so that the kinetic energy of water is transferred to the wheels.

The law of conservation of energy must be obeyed during all forms of energy transformation. Without external energy supplies, unlimited amount of energy cannot be transferred from a system to its surroundings [14].

There are many ways to transform energy. By using a driveshaft, mechanical power can be transmitted directly. Traditional mechanical gears are able to control the speed, torque and direction of power source through specific gear ratio.

Hydraulic systems use liquid under pressure to transmit power; hydroelectric power generation facilities to harness natural water power to generate electricity. Pumping water (windmill pumps) is one possible method for energy storage.

Pneumatic systems use gasses under pressure to transmit power; compressed air is widely used to operate pneumatic tools in the industry. For example, a pneumatic wrench is used to remove and install automotive tires far more quickly than could be done manually.

3.2 Magnetic Gears: History and Development

The idea of magnetic gears (MG) can be traced back to the early 20th century. In 1913, a US Patent [15] proposed a rudimentary topology of electromagnetic gears. This novel topology did not attract attention at that time since it looked remarkably different from traditional gear systems. Since 1941, people started to pay attention to MGs because of another US Patent [16]. But the poor properties of ferrite permanent

magnets such as low mechanical and magnetic strength limited the development of MGs. Improper topology also contributed to the less widely use of MGs.

It was the advent of neodymium iron boron (NdFeB) magnets that brought the concern of MGs back to the public. A neodymium magnet is known to be the most commonly used type of rare-earth magnet, a permanent magnet made from an alloy of neodymium, iron and boron to form the $Nd_2Fe_{14}B$ tetragonal crystalline structure [17]. Because of their excellent performance, neodymium magnets are the most powerful type of permanent magnets that are applicable for commercial use and have taken the place of the counterparts of other magnets in many products.

Multiple kinds of magnetic gear systems have been reviewed in the literature [18-20]. The coaxial magnetic gears (CMGs–Figure 3.1) can provide additional magnetic levitation capabilities besides torque transmission [18]. CMGs have been explained in detail in the literature and compared to some other types of magnetic gears [19, 20]

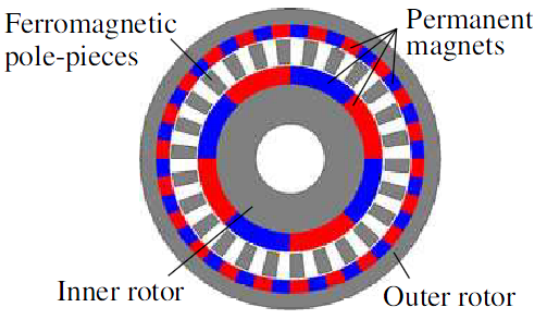

Figure 3.1 Coaxial magnetic gear.
Source: Abdel-Khalik AS, Ahmed S, Massoud A (2014) Alexandria Engineering Journal 53: 573-582.

3.3 Explanation of MARS

Magnetic Augmented Rotation System, US Patent No. 6356000 B1, was invented by Chun-Yuan Ho and Tien-See Chow and patented on Mar. 12th, 2002. The goal of the patent is to improve the efficiency of the drive wheel and prime mover. MARS includes several parts: wheel assembly, magnetic assembly, bearing assembly, magnetic biasing assembly and anti-reversing gear assembly. By specific geometry and topology, these components work systematically to transfer power from one wheel to another by magnetic coupling instead of mechanical contacts. Figure 3.2 is the schematic of MARS.

As shown in Figure 3.2, the MARS 10 is generally comprised of a wheel assembly 20, a bearing assembly 30, a magnetic biasing assembly 40 and an anti-reversing assembly 70.

The wheel assembly 20, contains a central portion 22, a first magnetic assembly 25, and a second magnetic assembly 26. The first and the second magnetic assembly, 25 and 26, respectively, have opposite polarity to each other.

The first magnetic assembly 25 is one magnetic disk linked to the center portion 22. It is aligned to make sure the surface 27 of the first assembly 25 has one magnetic polarity. Similarly surface 28 of another magnetic assembly 26 is aligned but with the opposite magnetic polarity.

In the lower part of Figure 3.2, in the wheel assembly 20, the magnetic assembly 25 is coupled with equally distributed and aligned magnets 75. The

alignment of magnets 75 on the second magnetic assembly 26 is completely asymmetrical to 25 along the central portion 22.

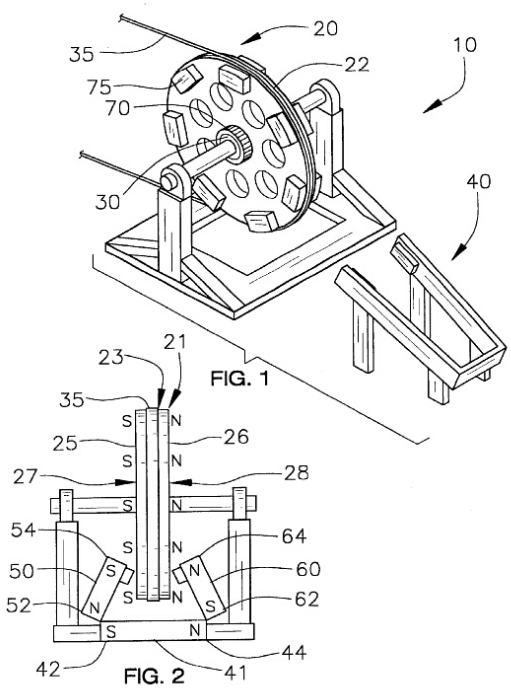

Figure 3.2 Schematic perspective view of MARS.
Source: Ho C-Y, Chow T-S (2002), Magnetically Augmented Rotation System, U.S. Patent 6356000 B1.

Annular grooves 23 are placed around the circumference of the central portion 22 of the wheel assembly 20.

A drive belt/train 35 is positioned in the annular groove 23 and transfers a primary rotational force to the wheel assembly 20.

The bearing assembly is made of non-magnetic materials and facilitates the rotation of the wheel assembly 20.

The magnetic biasing assembly 40 will apply torque to the wheel assembly 20 by the interaction between the magnetic biasing assembly 40 and the two magnetic assemblies 25 and 26. Three linear magnets are involved in the magnetic biasing - a first linear magnet 41, a second linear magnet 50, and a third linear magnet 60. The first linear magnet 41 is placed perpendicular to the surfaces 27 and 28. Also 41 is perpendicular to the circumferential edge 21 of the wheel assembly 20.

The second linear magnet 50 is placed next to one end 42 of the first magnet 41. There is an oblique angle between 50 and 25 where 50 rises upwardly to the first magnetic assembly 25 of the wheel assembly 20 and the other end 54 is contiguous to the surface 27.

The third linear magnet is placed adjacent to the other end 44 of the first linear magnet 41. It is symmetrical to the alignment of the second linear magnet 50 with the plane that is perpendicular to the first linear magnet 41 and passing through its mid-point.

The first linear magnet 41 is magnetized and one end 42 has one polarity (North Pole) while the other end 44 has the other polarity (South Pole). The two ends of the second linear magnet 52 and 54 have north and south poles, respectively. Ends 64 and 62 of the third magnet have north and south poles, respectively.

Above structures maintain repelling forces between the first linear magnet 50 and the first magnetic assembly 25, the second linear magnet 60 and the second magnetic assembly 26 according to corresponding polarities.

The anti-reversing gear assembly 70 is connected to the wheel assembly 20. It allows the MARS 10, to only rotate in one direction.

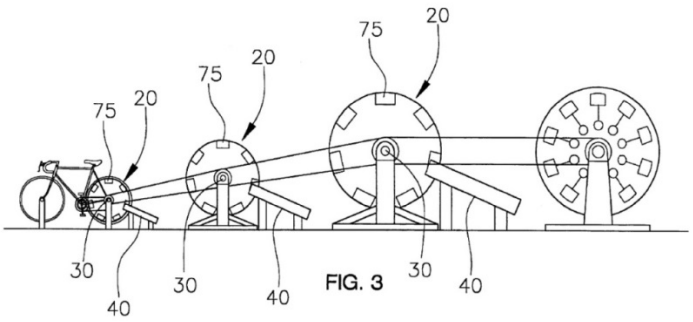

Figure 3.3 Schematic view of multiple embodiments of MARS in a cascade arrangement.
Source: Ho C-Y, Chow T-S (2002), Magnetically Augmented Rotation System, U.S. Patent 6356000 B1.

Figure 3.3 is a schematic view of multiple embodiments of the invention in a cascade arrangement. With the involvement of MARS, power could be transmitted from the magnetic driver to the magnetic rotor by magnetic coupling.

The bicycle on the left is analog to power input, and on the far right, the plate means the load. The two parts in the middle are MARS with same linear velocity but different angular velocity. By adjusting the parameters in MARS, velocity is controllable in the transmission system.

The MARS is an excellent option for pollution-free applications in solid state lighting, electric vehicles, self-sustained wheel chairs and small scale wind turbines etc. Wind power, hydro power and hand-held power are all regarded as compatible power input to drive the MARS and the power output is scalable and controllable [21]. For example, the electric charger on cars and trucks is usually 12 Volts or 24 Volts

and these voltage specifications can be achieved by using MARS-based sustainable energy generation method so that the traditional fossil fuel combustion will be substituted for direct-drive devices that convert mechanical sources of power into electricity while the vehicles are in motion.

Figure 3.4 is a prototype of MARS. This system is coupled with magnetic forces of repulsion. This will help to design a turbine that is facilitated by intelligent manipulation of magnetic fields. The other application of this technology will be in the form of a standard generator. The driver and driven wheel are made of copper. The driver wheel will be driven by the prime mover, such as wind power. The small rotor on the right is the driven wheel which consists of a number of magnets to increase the rotational speed of the rotor to be compatible with the rated generator. Due to the rotation of the magnets, there will be a constant flux change at the coils. Because of this, an electro motive force (EMF) will be generated. It is anticipated that MARS will improve the performance and efficiency of the drive wheel as a prime mover without the meshing and friction in traditional gears.

3.4 Optimization of MARS

As an extension of MARS, an improved contactless gear system has been designed and constructed in the laboratory. As is shown in Figure 3.5, each of the two wheels would act as the driver; when power input is applied to one wheel, the other one moves accordingly by magnetic coupling.

In this approach, a set of small round magnets are implemented on each of the two aluminum plates. Because every magnet has magnetic poles inward and outward, the magnets with different poles will attract each other. To utilize the repelling magnetic force between the two wheels, the outward surface of magnets of the upper wheel must have same magnetic polarity with that of the lower wheel. The uniformly distributed magnets will enable the torque and energy transmission more smoothly than with the material induced friction, energy ripples and energy loss that is associated with traditional mechanical gears.

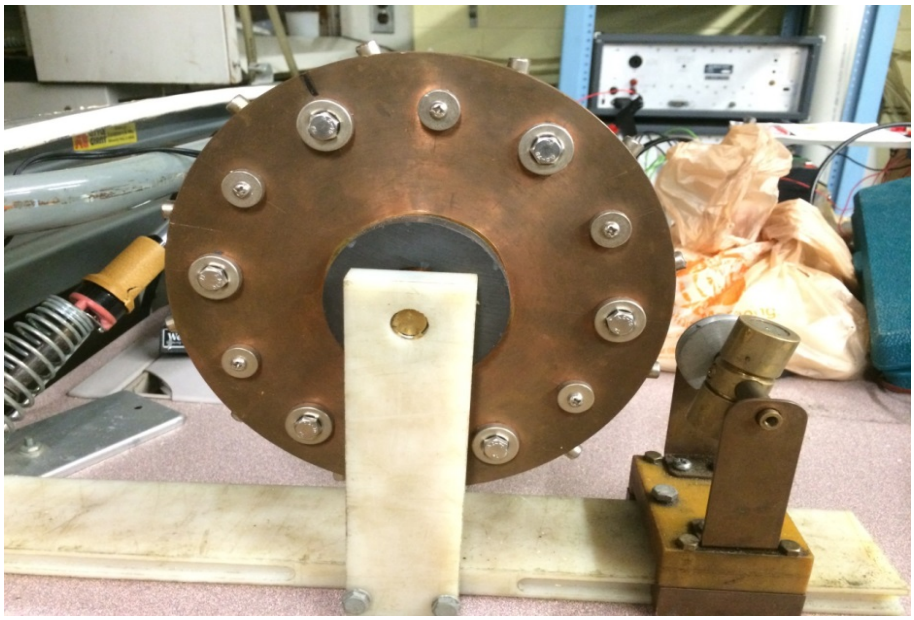

Figure 3.4 MARS prototype.

When one wheel is applied torque from power input, the other wheel will start rotating at the same time, but along the opposite direction. For example, when the drive wheel is moving along the clockwise direction, the driven wheel is moving anticlockwise.

The reason to choose aluminum as the substrate for MARS is mainly because of its low permeability and low density. Low permeability means that the aluminum plate will bring minimum effect on the interaction between magnets on both wheels. Low density exemplifies the low cost. Since the two aluminum plates should be produced as thin disks, the good malleability of aluminum is also a factor that is taken into consideration.

Figure 3.5 Contactless gear system.

Figure 3.6 is a picture of an optimized prototype of MARS. There are several modifications in this machine. First, the foundation of MARS is made heavier than that shown in Figure 3.4 to increase the stability of the system and avoid resonance. Second, a DC electric motor which will be used to simulate and measure input power is in place. The adjustable base and switch is implemented to facilitate the

controllability of the motor. Third, a low-Wattage bulb is used to imitate the actual load whose voltage, current and power are measurable.

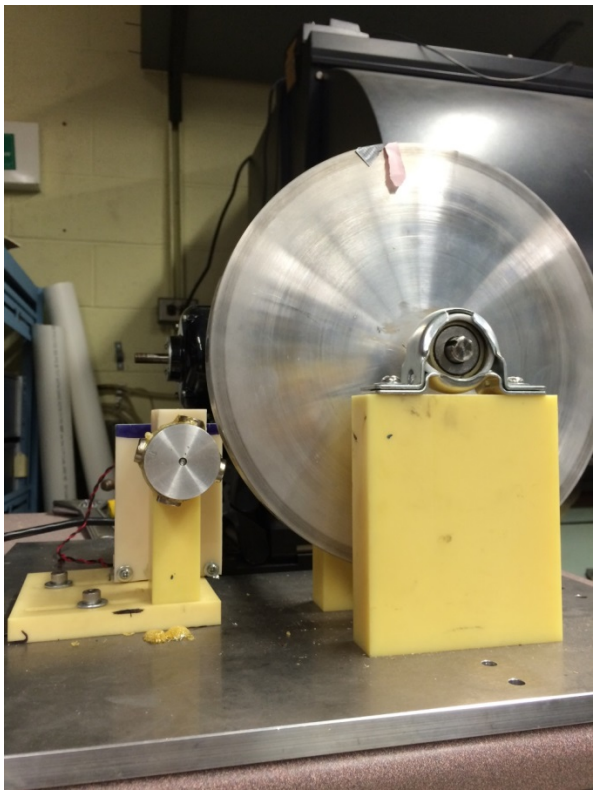

Figure 3.6 Optimized prototype of MARS.

3.5 Contactless Gears versus Traditional Gears

Compared to mechanical gears, Contactless Gears have a series of advantages. First, there is an air gap between the two wheels that eliminates the friction between the two wheels. No energy will be lost during rotation and thus the power transmission efficiency. Second, using rare earth permanent magnets, such NdFeB, will greatly reduce the weight; no bearing or lubrication will be added or replaced so that both the manufacture and maintenance cost will be reduced. Third, without the contact of the

driver and driven wheels, less noise and vibration will be produced. This feature will minimize the environmental disturbance of MARS. Next, the input and output shaft can be completely isolated and sealed which is a good option in fluid delivery system to avoid leakage. Moreover, MARS can tolerate misalignment of magnet poles. When the misalignment happens, the neighboring pairs of magnets will be matched and aligned again because of magnetic coupling. It has overload protection characteristics which will slip when the load is faulty so that the system will not suffer any damage under malfunction or emergency situation.

Limitations of MARS lie in several areas. First, magnets may not be as strong as materials used in mechanical gears so they may be subject to damage or fatigue due to high load or cyclic load. Second, MARS has low torque transmission capacity, which means when the load is larger than the maximum, "overload protection" mechanism of MARS will be activated; thus the drive train will stop working because the magnetic strength is not strong enough. Next, Curie temperature will restrict the utilization of MARS in extreme working conditions such as very high temperatures. Table 3.1 lists the benefits and limitations of Contactless Gears compared to mechanical gears.

Table 3.1 Benefits and Limitations of Contactless Gears

Benefits	Limitations
No friction and higher efficiency	Less magnetic field strength
Less noise and low vibration	Low torque transmission capacity
Low weight and less maintenance cost	Curie temperature restriction
Isolated input and output shafts	
Misalignment tolerance and overload protection	

CHAPTER 4

DESIGN AND CONSTRUCTION OF WIND TURBINES

The wind turbine is one of the most significant applications of MARS. In this chapter, the fundamentals of windmills will be introduced. Some issues of wind turbines will be discussed. Parameters that are involved in designing MARS based wind turbines are summarized.

4.1 Classification of Wind Turbines

Wind energy is one of the alternatives to conventional fossil fuels such as coal, petroleum and natural gas. Wind turbines are effective approaches to capture such renewable and clean power. They can be classified into two different methods: Installation regions and Axis alignment direction.

4.1.1 By Installation Regions

Onshore wind turbines are considered as traditional windmills that are usually installed inland, especially in remote plains or mountainous areas. In order to increase the wind power generation capacity, groups of onshore wind turbines can be installed intensively and work cooperatively as a wind farm. Power generated by onshore wind farms is able to not only supplement the electricity grid but can also be the source of power for isolated, off-grid areas [22]. Low construction costs and easy acquisition of wind energy in windy areas are the reasons for the consumers to be able to access

affordable electricity from onshore wind power since such electricity is generated less expensively than those from offshore wind power or solar panels. Though such electricity has higher price than that produced by fossil fuel, it is promising that the price of the electricity will decrease with the advancements of technology.

Offshore windmills refer to the wind turbines that are built in water bodies, especially in the lakes or oceans. Compared to onshore wind power, high annual average wind speed at sea provides the more intense and less variant wind resource in the near-sea oceanic areas. Because of the long coastlines available for extraction of offshore wind power, many nations such as China and the United States have abundant potential in offshore wind power utilization. Though the current offshore proportion of wind energy utilization is only less than 2% of 94GW total capacity [23], great interest is shown in offshore windmills development all over the world. For example, Denmark has currently about 2300 MW of wind power capacity distributed throughout the power system in onshore and small-scale offshore settings. Since 2000, large-scale offshore wind farms have been announced and planned to incorporate about 4100 MW of offshore power capacity. This will correspond to about 40% of Danish electricity consumption [24]. Offshore windmills have advantages over fossil fuel plants and onshore windmills in many fields. For example, they create less noise to residents, longer blades and higher capacities and less impact on animals than onshore windmills.

The major challenge faced with offshore wind turbines is the high cost in both construction and operation aspects. Increased distance from the shore and depth from the sea level will result in high costs. Additionally, inclement weather conditions such as thunderstorm and lightening require costly maintenance and precautions, not to mention saline corrosion which requires protection layer on all surfaces of each windmill. All these factors increase the price of offshore electricity; this weakens the competiveness of offshore windmills compared to their onshore counterpart [25].

4.1.2 By Rotation Axis Orientation

Wind turbines can rotate around either a horizontal axis or a vertical one. The Horizontal Axis Wind Turbine (HAWT) is a conventional and common form of windmills. Usually HAWT has a huge supporting tower and a long pole with the main rotor shaft, the generator and gearbox on the top. The blades extract the kinetic energy of the wind. The gearbox accelerates the speed of rotation of the blades in order to drive the generator to produce electricity. To ensure that the motion of the plane of the turbine blades is directly facing the wind, wind vane or wind sensor must be installed. The tower, the pole and blades have to be strong and stiff enough to prevent damage caused by fierce wind. HAWTs often contain three or more blades to maximize their wind capture ability and they are often of upwind design to minimize turbulence. High efficiency and low torque ripple provide reliability of HAWTs, and modern, unconventional HAWTs keep evolving in the 21st century. The common height of the tower is above 50 meters and the length of a blade is around 30 meters. However,

tendency towards large scale inevitably increases the weight and the high standards of building materials which add burden to the construction costs.

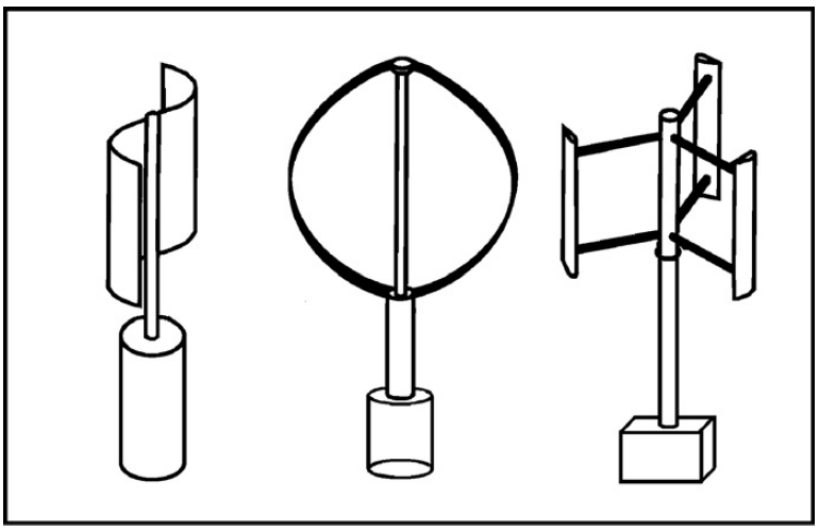

Figure 4.1 Three different types of VAWTs (from left to right: Savonius, Darrieus, and H-rotor).
Source: Eriksson S, Bernhoff H, Leijon M (2008) Evaluation of Different Turbine Concepts for Wind Power, Renew Sust Energ Rev 12: 1419-1434.

Vertical Axis Wind Turbine (VAWT) is another form of wind turbines in which the blades rotate around a vertical axis. There are several types of early design of VAWTs. For example, in 1922, S.J. Savonius invented the Savonius turbine. Later, aeronautical engineer Georges Darrieus designed a VAWT using bent blades, called the Darrieus wind turbine. H-rotor wind turbine is usually referred to as the straight-bladed, but has also been called giromill or cycloturbine.

There are a number of differences between HAWTs and VAWTs [26]. Compared to HAWTs, blades of VAWTs can begin to rotate in any direction of wind so that VAWTs are suitable for places with highly variable winds. Moreover, unlike

HAWTs, the generator and gearbox can be placed at the bottom instead of the top, reducing the construction, operation and maintenance costs.

Major problems limit the wide use of VAWTs. First, the fatigue of blades would result in the failure, malfunction or damage to the whole turbine system. Egg-beater design in shape could decrease the centrifugal stress on the mechanism. By providing helical twist and torque variation during operation, bending moments on the blades will be reduced. Second, low rotational speed and inherently lower power coefficient compared to HAWTs remain unsolved. Particularly when referring to the megawatts order, VAWTs face the incapability of utilization of the lower part of blades since they are too close to the ground to generate power. Third, it is even more challenging to model and simulate the wind flow and the motion of the rotor accurately when designing these systems.

4.2 Problems and Issues in Wind Turbines

4.2.1 Noise

Noise pollution is among the most significant issues that hinder the public acceptance of wind turbine installation and operation. In the World Health Organization report, it has been reported that 55 dB(A) and 50 dB(A) can cause serious and moderate annoyance during daytime and evening, respectively. Particularly, at night time, 40 dB (A) and 30 dB (A) represent the maximum limit of the outdoor and indoor sound levels to avoid sleep disturbance, respectively [27]. Excessive noise produced by wind

turbines may disturb the sleeping of residents nearby, damage the hearing capability of people and affect other parts of human bodies.

There are two major noise emission sources of wind turbines. One is called as the mechanical source and the other is the aerodynamic source. Motion and interaction between moving mechanical parts such as gears in the gearbox can cause the noise. Improvements in drivetrain system against sound and vibration would help to cut down the mechanical noise. The aerodynamic noise remains a big problem to noise removal since it is affected by many factors such as airfoil shape, air flow speed and the rotor tip-speed ratio.

In Table 4.1, the maximum limit of noise produced by wind turbines are summarized [28]. The aim of such maximum limit is to protect residents from disturbance and annoyance from the wind turbine noise. But the limit restricts the maximum operation output power at the same time so that wind turbine manufactures and researchers are required to fully understand the cause of noise generation and make innovations and improvements to noise reduction and insulation technology. For example, flax fiber reinforced materials are proven to be a good candidate in sound and vibration removal due to outstanding damping absorption coefficient [29].

4.2.2 Energy Loss

In traditional power transmission systems such as mechanical gearboxes, cooling medium is needed to dissipate the heat generated by friction from inside to outside. The power loss in the gearbox is comprised of gear, bearing, seal and ancillary losses.

Gear and bearing losses contain load-free and load losses. Load-free losses are caused by rotation of mechanical parts even if no torque transmission occurs. These losses are also associated with operating conditions, lubricant conditions etc. Load losses occur during contact of power transmission components and depend on transmitted torque, coefficient of friction or rolling and lubrication condition [30].

Table 4.1 Wind Turbine Noise Limits in Some Countries

Country	Daytime Noise Limit dB (A)	Nighttime Noise Limit dB (A)
PR China	50	40
USA	45	35
Germany	50	35
Spain	45	45
India	55	45
UK	Ambient Noise +5	Ambient Noise +5
Italy	55	45
France	Ambient Noise +5	Ambient Noise +3
Canada	50	40
Denmark	40	40

Source: Shaltout ML, Yan Z, Dushyant Palejiya, Chen D (2015) Tradeoff Analysis of Energy Harvesting and Noise Emission for Distributed Wind Turbines, Sustainable Energy Technologies and Assessments 10: 12-21.

Mechanical components such as bearings and gears are constantly working in applications requiring material wear, abrasion, rolling and friction. To handle these tough working conditions and guarantee the good reliability and lifespan, special attention should be paid to the operation and maintenance in both regular and emergency situations, especially in the drivetrain system of wind turbines. Failures in the drivetrain system may lead to severe damage to core components of wind turbines. Such damage will call for the least desirable situations: expensive repairs and loss of

downtime. By SEM images and fractography, white etching area were found near the surface showing microstructural transformation, sometimes severe plastic deformation occurred in these areas. These transformation or deformation may lead to the failure of drivetrain [31].

4.2.3 Influence of the Environment

To obtain optimal wind condition and minimal interference to residents, wind turbines are usually built far away from urban areas. Onshore wind farms, which may be installed in mountainous or sandy areas, are exposed to sands and stones carried in the winds that will exacerbate the abrasion and wear in the drivetrain and surfaces of wind turbines. Abrasive particles erode blades and reduce the surface smoothness, thus deteriorating the aerodynamic performance. In hot and humid areas, insect collision and contamination is a big challenge. It will foul the leading edge and cause the power output to decline [32].

In cold climate, ice formation and adhesion is a significant problem to wind turbines. Extra load on turbine blades will likely decrease their fatigue life. Cold temperature may make contributions to mechanical strength degradation. Ice throwing may cause even personal injury or property loss in the vicinity of wind turbines. Heavy icing would possibly lead to full stop of the wind turbines. In warmer and humid regions, there is a huge population of insects. Insect collision with blades will foul the surface of turbine blades and reduce the power of the turbine. In arid or desert environment, sand particles may aggravate the wear and abrasion of blade surfaces. In

oceanic offshore areas, chemical corrosion is an inevitable tough problem to solve. These detrimental problems challenge the operation, maintenance and profitability of wind turbines.

One of some effective solutions to above issues is focusing on coatings. Special coatings offer adhesion alleviation leading to low friction, non-stick and smooth surfaces which are difficult for insects or sand particles to adsorb. Even if adsorption is initiated on the surface, it would be easily removed by shear force due to the weak bonding between contaminants and turbine blades with the existence of coatings. StaClean was reported as a highly recognized antifreezing coating that is used to reduce ice formation and adhesion on turbine blades [33].

4.3 Aerodynamics of Wind Turbines

Aerodynamics of wind turbines is important in the process of wind turbine design and manufacture. Some fundamental aerodynamic laws and parameters are presented below to help design a well performing wind turbine.

4.3.1 Power Coefficient and Betz's Law

In aerodynamics, extractable power of wind turbine is expressed by the following equation [34]:

$$P_r = \frac{1}{2} C_p A \rho v^3 \tag{4.1}$$

where P_r is the rotor power of turbine blade, C_p is the power coefficient, A is the swept area of blades, ρ is the air density, v is the wind speed. From the above equation, it is concluded that the power extracted from wind is positively correlated to some critical variables: power coefficient(C_p), square of turbine blade radius(R^2), air density(ρ), and cube of wind speed(v^3).

Power coefficient measures how efficiently the wind turbines convert kinetic energy in the wind into electricity:

$$C_p = \frac{Rotor\ Power}{Total\ Available\ Energy\ in\ the\ wind} = \frac{P_r}{\frac{1}{2}A\rho v^3} \quad (4.2)$$

But the range of wind energy utilization is confined by Betz's law. Betz's law defines the upper limit of kinetic power that can be extracted from wind. In 1919, German physicist Albert Betz argued that regardless of the kind of wind turbine design, no more than 16/27 (59.3%) of kinetic energy of wind will be captured [35]. The factor 16/27(0.593) is called Betz's coefficient or Betz's limit and the modern wind turbines can achieve 70-80% of the Betz's limit at most.

4.3.2 Lift and Drag Force

When airflow travels over an airfoil, there are two aerodynamic forces. Lift force is perpendicular to the direction of wind while the drag force is parallel to the wind direction**.** These forces are the driving forces for the rotation of wind turbines.

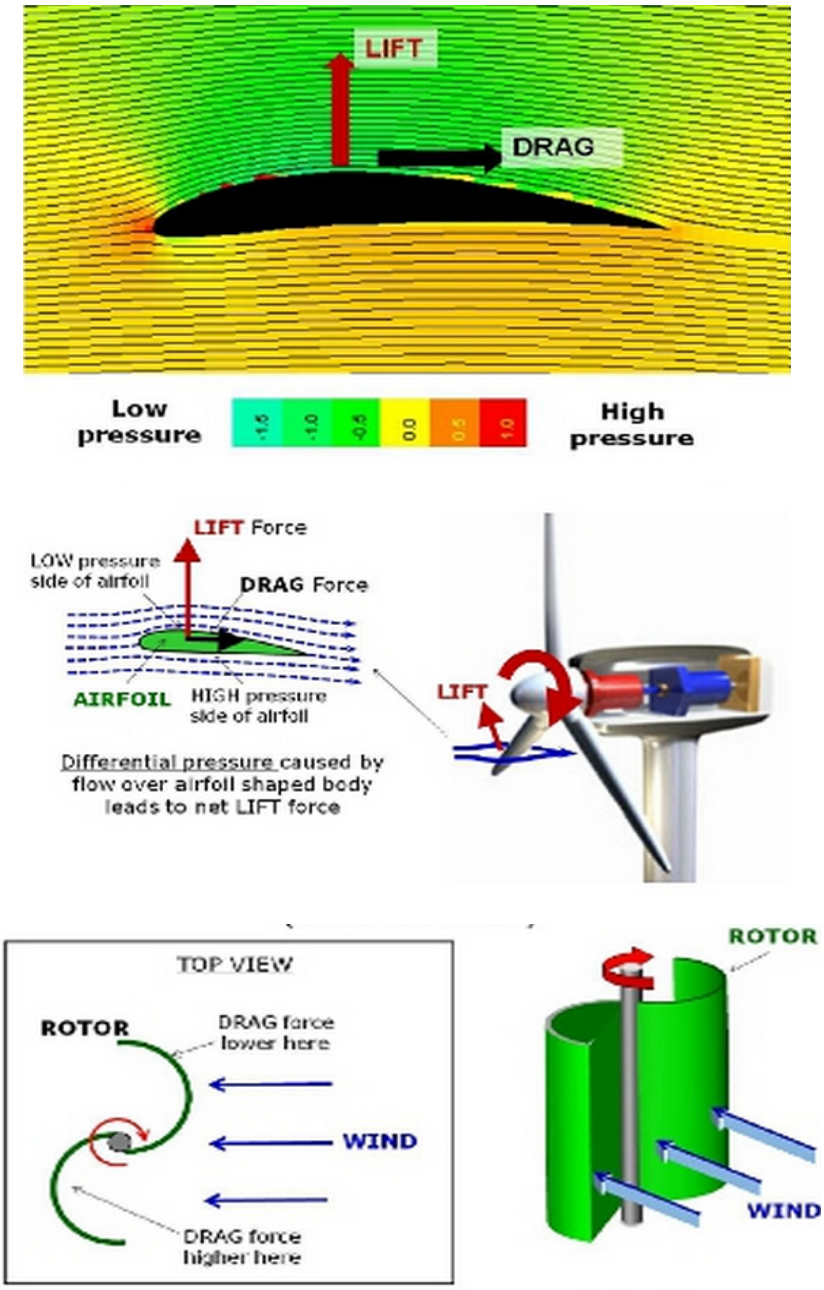

Figure 4.2 Schematic illustration of lift and drag.

Source: Department of Mechanical Engineering at Boston University, Lift and Drag, http://people.bu.edu/dew11/liftanddrag.html. Accessed 04/18/2015.

In the research entitled Lift and Drag in Mechanical Engineering Department at Boston University (as is shown in Figure 4.2), the two forces are shown and explained [36]. Jet plane wings, as in the upper image, will have different pressure on their top and bottom faces according to specific streamline design. The air above the

wing moves faster than that under the wing; so lower pressure will be on the top side. As a result, the net force applied on the wing will “lift” the plane. In the middle image, HAWTs are lift-based wind turbines. Pitch angles should be controlled well to set the blades within steady speed range. In the lower image, a Savonius VAWT is shown as a drag-based wind turbine. Since the drag force is larger on the concave face of the blades than on the convex face, the net drag force drives the turbine to rotate.

4.3.3 Variables in Wind Turbine Power Output

Rotor power will be transmitted to the generator through transmission systems with the mechanical efficiency, η_m, and then the mechanical energy will be converted into electricity, with the generator efficiency, η_g. Finally, electrical power output of wind turbines, P_e, is expressed as [35]:

$$P_e = \eta_g \eta_m P_r = \frac{1}{2} C_p \eta_g \eta_m A \rho v^3 \tag{4.3}$$

The power coefficient represents the aerodynamic efficiency of the wind turbine and is a function of the tip speed ratio, λ, which is defined as the ratio of speed at the tip of the blade to the wind speed [37]:

$$\lambda = \frac{\omega R}{v} \tag{4.4}$$

where ω is the angular velocity of the turbine blade, R is the radius of the blades, and v is the wind speed. Based on theoretical studies and experimental results,

C_p values for HAWTs are usually around 0.40, within the range of 0.40 and 0.50. Power curves of three different turbines are shown in Figure 4.3. The VAWTs have good efficiency as the HAWTs, but the higher C_p value for the HAWTs may be due to the more optimized design [26].

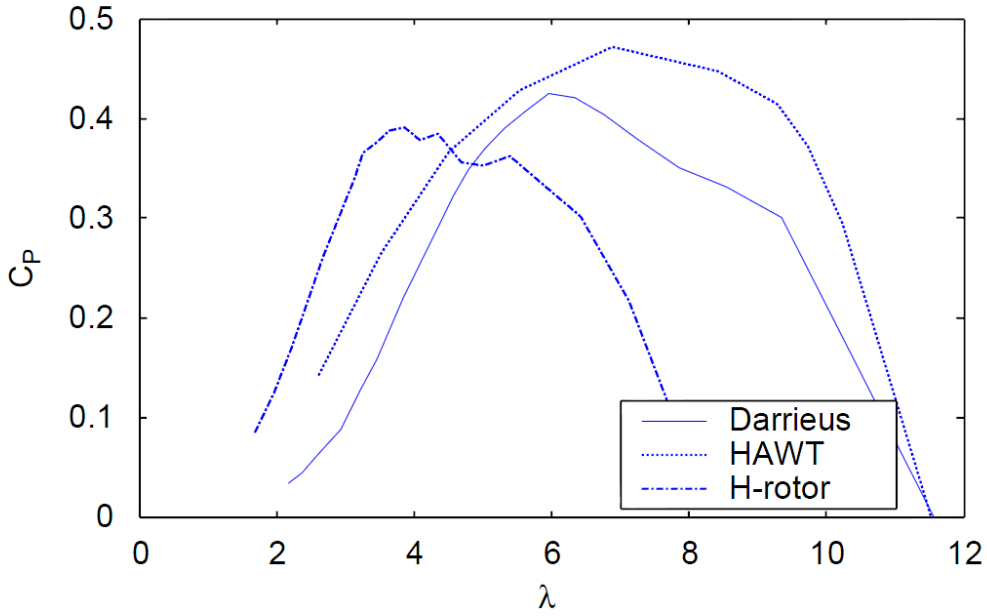

Figure 4.3 Power curves for the different types of turbines, as function of λ.
Source: Eriksson S, Bernhoff H, Leijon M (2008) Evaluation of Different Turbine Concepts for Wind Power, Renew Sust Energ Rev 12: 1419-1434.

The turbine blade is normally designed at a fixed speed but from the figure above, it is shown the fixed speed wind turbine is not operating at peak efficiency across a range of wind speeds. Instead, only one value of λ could achieve the highest power coefficient. The desire for maximum efficiency in the entire wind speed range is thus a diving force for the development of variable speed wind turbines.

The solidity, σ, expresses a relation between the blade area and the turbine swept area and has different definitions for different types of turbines [26]. For a HAWT, it is defined as:

$$\sigma = \frac{Bc}{\pi R} \tag{4.5}$$

where B is the number of blades, c is the chord length, and R is the radius of the turbine. For a VAWT, the solidity is defined as:

$$\sigma = \frac{Bc}{R} \tag{4.6}$$

With low solidity (0.10), rotor runs at high speed and lower torque, while with high solidity (>0.80), rotor rotates at lower speed and higher torque.

Air density can be calculated according to a molar form of the ideal gas law:

$$\rho = \frac{PM}{RT} \tag{4.7}$$

where P is the absolute pressure shown in SI units, M is molar mass, R is ideal gas constant and T is the absolute temperature. In places with higher atmospheric pressure, cold temperature and lower humidity, the air density will be larger than those hot, humid areas with low air pressure.

Power output is proportional to the square of radius of wind turbine blade, R. Hence, the larger the size, the more energy the turbine blades will capture.

In wind turbine engineering, an exponential relation between wind speed and height is expressed with respect to a reference height of 10 meters as [38]:

$$v_w(h) = v_{10}(\frac{h}{h_{10}})^{\alpha} \tag{4.8}$$

where $v_w(h)$ is the velocity of the wind at height, h,. v_{10} is the velocity of the wind at height of 10 meters, h_{10} equals to 10 meters, α is called Hellmann exponent, which is location specific. Examples of values are listed in Table 4.2 [39].

Table 4.2 Example Values of Hellmann Exponent

Location	α
Unstable air above open water surface	0.06
Neutral air above open water surface	0.10
Unstable air above flat open coast	0.11
Neutral air above flat open coast	0.16
Stable air above open water surface	0.27
Unstable air above human inhabited areas	0.27
Neutral air above human inhabited areas	0.34
Stable air above flat open coast	0.40
Stable air above human inhabited areas	0.60

Source: Kaltschmitt M, Streicher W, Wiese A (2007) Renewable Energy: Technology, Economics and Environment. Springer Science & Business Media, New York, NY, USA, p 55.

The power output is in direct proportion to cube of wind speed. Wind speed v, depends on altitude and friction. When the altitude is elevated, the atmospheric pressure and friction due to viscosity of air are reduced, thus increasing the speed. In

mountainous, oceanic areas and plains, the annual average wind velocity is often higher than other regions; so they are advantageous to set up wind farms for electricity conversion.

4.4 Wind Turbine Design

To design a wind turbine, a series of factors need careful considerations; for example, choosing the size of the turbine, materials properties, turbine structure, power control methods and cost control. The design usually focuses on the topology of a wind turbine, as shown in Figure 4.4. A good structure will not only improve the efficiency and power output of wind turbines but also reduce the corresponding cost.

4.4.1 Capacity Analysis

Wind turbines acting as utility supply are very large to provide enough power. Currently, such turbines have power ratings as high as megawatts. In 2014, Vestas claimed their biggest wind turbine with capacity up to 8-megawatts, 80-meter-long blades and 21000 m^2 swept area. These turbines are installed and arrayed as wind farms, as the developed infrastructure would provide convenience in the management of turbines [40].

Wind turbines for utility loads or remote communities are usually in smaller scale, ranging from 10kW to 200kW. Installation and maintenance convenience would be the priority when designing such turbines.

4.4.2 Topology

Table 4.3 describes the topology of wind turbine design. The choice of options depends on location-specific conditions and desired goals for wind turbines.

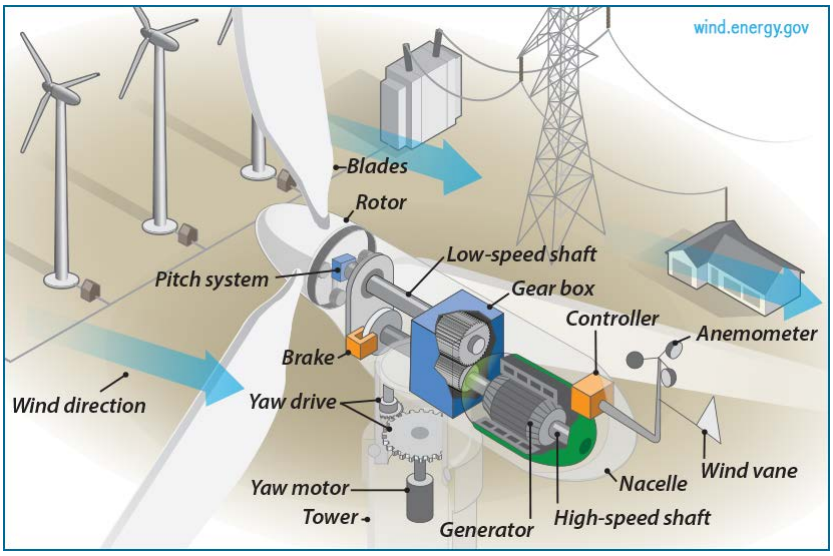

Figure 4.4 Structure of a HAWT.
Source: U.S. Department of Energy, The Inside of A Wind Turbine, http://energy.gov/eere/wind/inside-wind-turbine-0, Accessed 04/19/2015.

The determination of the rotor axis orientation is the first and one of the most significant steps when choosing the components. The preference of choosing HAWTs over VAWTs is mainly due to the following reasons: first, at a given design tip speed ratio, the rotor solidity of HAWTs is lower than that of VAWTs; thus the total blade mass compared to swept area is lower so that the construction cost will be reduced. Second, the average height of the rotor swept area is higher; thus the blades can capture more wind energy.

The next component to be considered is the power control system. At high wind speeds, stall-controlled wind turbines can reduce their aerodynamic lift by adjusting the angles of attack [41]. When the maximum power arrives at very high speeds, the stall begins to function. The drive train should fit well for the torques faced under those conditions, irrespective of the frequency. The mechanical systems should be always incorporated to make sure that the turbine could be turned off under any circumstance, especially under overload condition.

Table 4.3 Topology of Wind Turbine Design

Components	*Options*
Rotation axis	Horizontal or vertical
Power control	Stall, variable pitch, controllable aerodynamic surfaces etc.
Rotor position	Upwind or downwind of the tower
Yaw control	Driven yaw, free yaw or fixed yaw
Rotor speed	Constant or variable
Tip ratio and solidity	Depending on desired aerodynamic goals
Type of hub	Rigid, teetering, hinged or gimbaled
Number of blades	One, two, three or above three
Tower structure	Stiff, soft, or soft-soft

Source: Manwell JF, McGowan JG, Rogers AL (2010) Wind Energy Explained: Theory, Design and Application. John Wiley & Sons, New York, NY, USA.

Variable pitch control wind turbines can change the pitch angle of their blades. The angle of attack and the torque generated will also be altered due to the pitch change so that the maximum electrical load will be reduced when hurricanes occur [42]. Though the variable pitch control system offers more flexible control, the incorporation of pitch bearings and pitch actuation system increases its complexity

Aerodynamic surfaces will be used on the blades to manage power. Regardless of various forms, the surfaces should be fit for the blades and operation methods. Mostly, the aerodynamic surfaces are used to slow down the turbine.

Yaw control is another power control alternative. By yaw control, the rotor can face away from the wind to reduce the power. In downwind turbines, yaw motion is free and always points into the wind like a weather vane. Yaw dampers should be installed to control the yaw rate and the gyroscopic loads of the blades. Active yaw control system which contains a yaw motor, gears and a brake is more complicated and is usually adopted in upwind design to keep the turbine steady. Yaw control requires a strong yaw system and the hub should be able to bear gyroscopic loads resulting from yawing motion. The supporting systems such as the towers should be torsional load resistant when the yaw system is running.

Similar to a propeller driven airplane, the rotor of an upwind turbine is in the front of the tower and it is the most common type of small wind turbines in the U.S. Reduced tower shading would be its strength, but the blades themselves should be stiff enough and the distance between the blades and the nacelle should be kept wide enough to avoid blades hitting the tower. So the blades and the joints are highly stressed, especially in extreme weather conditions, which would result in shortened life of these components.

As the nacelle is designed to point into the wind, a yaw is unnecessary in downwind turbines. This downwind structure has a few advantages over the upwind

structure. First, the danger of the blade strike no longer exists. Second, they are less expensive to produce. Third, part of the stress on the tower could be transferred to the blades by the flexible blades. But the flexing could also fatigue the blades and tower shadow may cause turbulence, wake and electricity ripple.

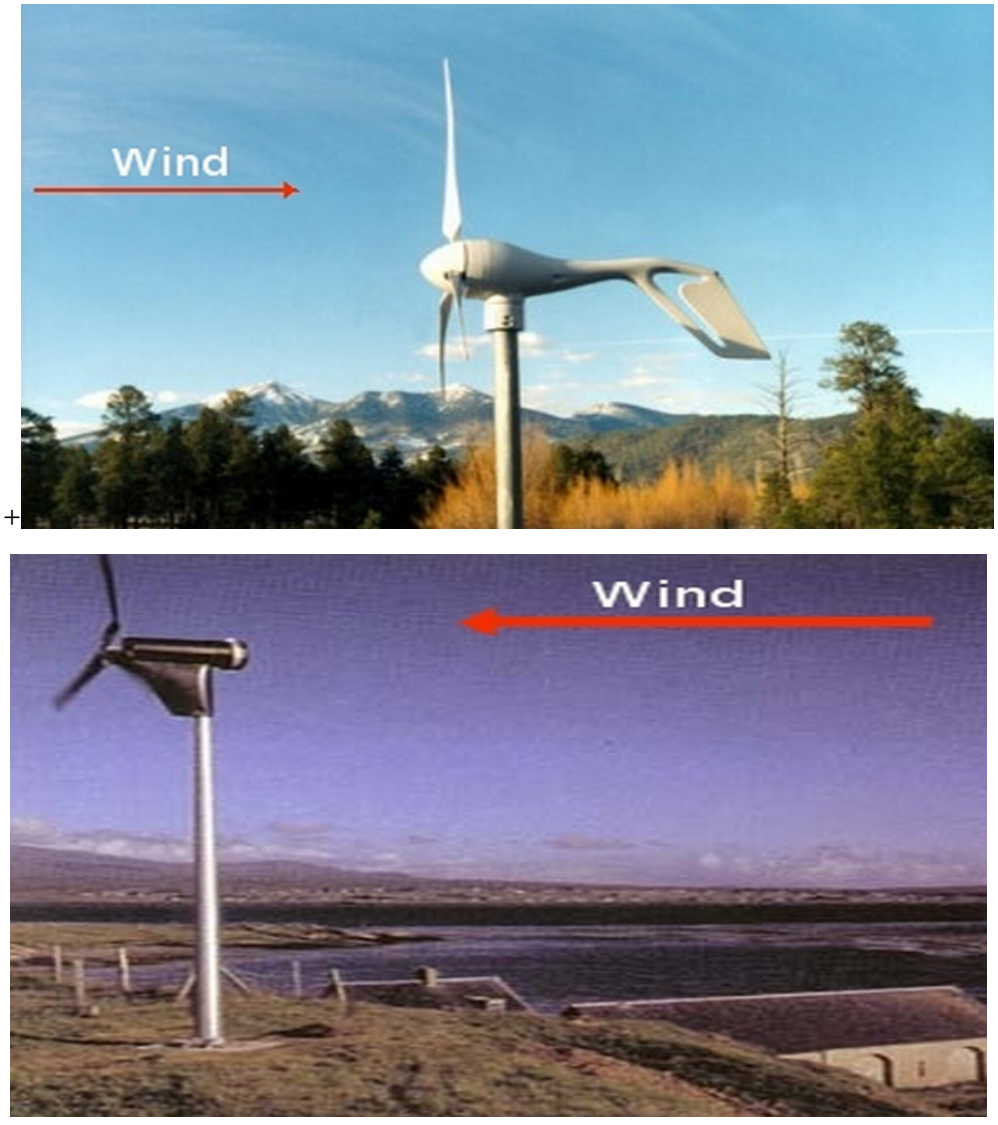

Figure 4.5 Upwind (upper) and downwind (lower) design of wind turbine rotor.
Source: Upwind Turbine Vs. Downwind, http://www.power-talk.net/upwind-turbine.html.
Accessed 04/20/2015.

Most grid-connected wind turbines choose constant rotational speed according to the electrical generator and the gearbox. In some cases, the rotor is able to work with the choice of constant or variable speed. For instance, the incorporated power electronic converters in most variable speed wind turbines could offer flexibility for the type of generator. The use of low speed generator could get rid of heavy gearbox, but electrical noise due to the converters is another derivative problem. The related issues according to the variable speed wind turbines should be considered when making the determination.

The goal of tip speed ratio is to find the proper tip ratio which would achieve the maximum power coefficient. The tip speed ratio has a strong influence on the whole design since it can decide the power coefficient, solidity and the swept area. For example, to get a fixed tip speed ratio, the swept area of a high speed rotor is less than that of a slow rotor. For a constant rotor speed, the tip speed ratio is only dependent on the wind speed. The number of blades is proportional to the solidity so that the decrease in solidity will lead to the decrease in the number of blades.

Higher tip speed ratio is preferred because of the following advantages. First, the less number of blades reduces the cost of blades. Then, higher rotational speed will reduce the torque at given power. Hence, the lower torque requires less compensation of the drive train. However, an accompanying problem is that high-speed rotors cause more noise than low-speed ones, which could be considered as one of the shortcomings of higher tip speed ratio wind turbine design.

Rigid, teetering and hinged hubs are the major three types of hub design. The rigid hub is the most widely used type, which prevents the blades from moving in the flapwise and edgewise directions, but still allows the variable pitch. Two-bladed rotors would probably choose teetering hubs. The hub is installed on bearings and it would point into or turn away from the upwind direction. The blades are rigidly connected to the hub, so when teetering is happening, one blade moves into upwind direction while the other moves downwind. This flexibility reduces the bending moments on the blades. Hinges on some two-bladed wind turbines even enable the blades to move into or out of the rotation plane independent of each other, but the balance of the blades' weight should be considered in this design.

Choosing the number of blades is a significant step in wind turbine design. A few one-bladed turbines have advantages of their relatively low costs and high tip-speed ratio. But the imbalance of blade weight and the aesthetic asymmetry may limit the development of these turbines. Two-bladed rotors still have the problems of imbalance of moment of inertia in different positions. It is harder to yaw the blades when they are aligned horizontally than vertically through teetering. The efficiency of two-bladed turbines is slightly lower than those with three or more blades. Three-bladed wind turbines are the most common modern turbines in electricity production because the polar moment of inertia remains constant when yawing and is free of azimuthal position. This feature leads to the smooth running of the turbine.

Though using more than three blades will increase the efficiency, such increase could not compensate for the cost of more blades. Moreover, the stress on the root of the blades will be increased with more blades, thus requiring stronger and more expensive materials. Therefore, those blades are less likely to be commercialized.

A tower is a crucial supporting component of a wind turbine. For HAWTs, the tower has to be high enough to lift the main part of the turbine aloft and prevent the blade tips from hitting the ground. In reality, the height of the towers should be as high as practical, as long as the economy of increased captured energy can offset the increasing cost. Despite the height, the tower should also be sufficiently stiff to resist the aerodynamic turbulence and resonance caused by the blade rotation when their natural frequencies are too close.

Three available types of towers are presented here. Stiff towers have higher natural frequency than blade passing frequency, rotors' rotational speed times the number of blades. These towers are blunt to the turbine motion but are heavy and expensive. The natural frequency of soft towers is higher than the blade passing frequency. Soft-soft towers have their natural frequency even lower than both the rotor frequency. The latter two soft towers are less expensive than the stiff ones because they are made of lighter materials, but attention should be drawn on them to avoid any resonance that could be excited. Tubular tower is one of the most prevalent tower structures because of its overall high stiffness and aesthetic preference.

4.4.3 Load Estimation

There are different types of loads in operation that wind turbines have to be able to withstand. These include regular loads for as long as possible and sometimes extreme weather conditions for a short period. Hence, an early estimation of future loads within the design section is necessary. The loads will perform as input data for the design. This process will be facilitated by useful computer-aided simulation engineering software to qualify for preset requirements. It can be modified and updated as the specifications of the whole turbine systems are detailed in later design. Table 4.4 lists the different types of load.

Table 4.4 Different Categories of Wind Turbine Loads

Load Categories	*Explanation*
Static	Not related to rotation
Steady	Related to rotation, e.g. centrifugal force
Cyclic	Wind shear, blade weight, yaw motion
Impulsive	Short duration loads, e.g. tower shadow effect
Stochastic	Turbulence
Transitory	Starting/Stopping
Resonance induced	Resonance near the natural frequency of whole system

Source: Manwell JF, McGowan JG, Rogers AL (2010) Wind Energy Explained: Theory, Design and Application. John Wiley & Sons, New York, NY, USA.

4.4.4 Preliminary Design

When the previous step is completed, detailed specifications of all subsystems will be designed. Wind turbines contain several subsystems. Principal components of each subsystem have to satisfy specific requirements. Table 4.5 lists the subsystems and their principal components.

4.4.5 Cost and Quality Control

Estimation of the cost of energy is one of the most significant parts of the wind turbine design. The estimation is essential to predict the cost of the turbine. Wind turbine components contain commercially available items and specially designed and fabricated items. The latter may have higher price in prototype design stage, but their price will decrease when entering mass production period.

Table 4.5 Wind Turbine Subsystems and Their Principal Components

Subsystems	*Principal Components*
Rotor	Blades, hub, aerodynamic surfaces
Drivetrain system	Shafts, couplings, gearbox, brakes, generator
Housing system	Nacelle
Direction control system	Yaw, Pitch control
Support system	Tower, foundation and erection

Refinement of preliminary design should be done after the performance evaluation to ensure that the design is strong enough for the loads and is close to the projected production capability. If it fails the target, the above five steps need to be repeated until the evaluation is satisfying.

4.4.6 Build and Test Prototype

A prototype should be constructed once the feasibility of the design has been proved. The prototype is used to test the hypothesis in the design, add possible novel ideas and make maximum effort to the successful fabrication, installation and operation of the wind turbine. A wide spectrum of field tests will be launched on the prototype, and

various gauges and instruments can be equipped to collect actual data, for example, the actual load and the final output power. Data will be analyzed to compare the performance of the prototype to the expectation.

4.4.7 Machine Design and Manufacture

End product-wind turbines should be as similar as the prototype, though slight modification and decoration are allowed to exist for safety, cost-saving and aesthetic purposes. It is also appropriate to choose the cost-effective, efficient and low-pollution fabrication methods when mass production is under way. These methods may have differences with those adopted in producing the prototype.

4.5 Prototype Construction

A prototype of wind turbine is built and shown in Figure 4.6. The foundation and tower are made of PVC tubes because of its high mechanical strength versus low weight, economy and good workability. The joints are chosen from different sizes of PVC components to fix and match the tubes. The tubes are hollow and can be filled with sand to increase their weight and thus the stability of the whole system. Four-bladed and smooth surface design is intended to increase the capability of wind energy capture. Rigid hub is adopted and covered outside the rotor axis. A generator is placed at the rear of the hub, thus making the turbine to be compatible with upwind design.

Figure 4.6 Prototype of the wind turbine.

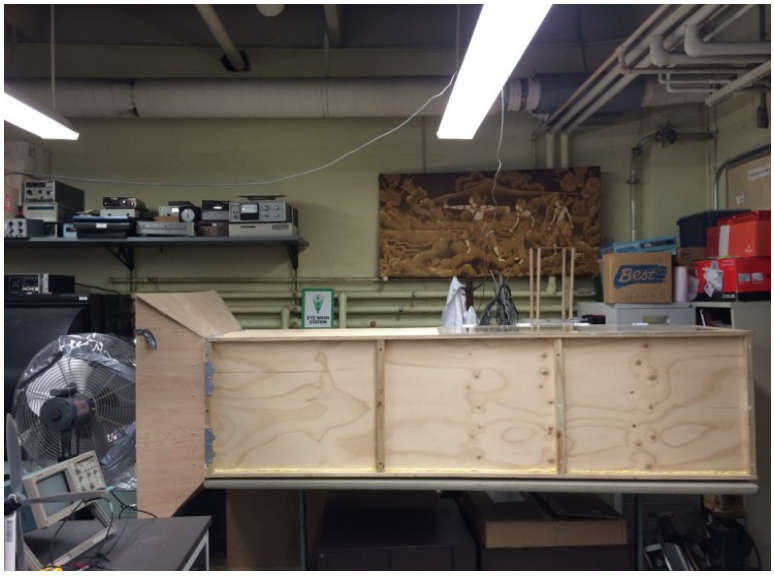

Figure 4.7 The wind tunnel used for wind turbine experiments.

A wind tunnel (see Figure 4.7) is built to obtain a steady average wind speed. The tunnel is made of wood and is interfaced with an electric fan which acts as the wind source. A mesh is installed in the tunnel near the entrance to regulate the wind. Laminar flow environment is approached in the middle of the tunnel. As is shown in Figure 4.8, an anemometer is installed on an adjustable rack to locate the most stable and maximum average wind speed. A mobile transparent glass board is covered on the top of the tunnel to observe the reading of the anemometer. A low-Wattage bulb is connected to the turbine and an oscilloscope to measure the current pattern generated by rotation of this wind turbine. Calculations and results will be presented in the next chapter.

Figure 4.8 The wind turbine prototype in the wind tunnel.

CHAPTER 5

CHARACTERIZATION OF MARS BASED WIND TURBINE

5.1 Wind Tunnel Experiments

Figure 5.1 An electric fan connected to the suction with plastic foils at the entrance of the wind tunnel, serving as wind source.

To further investigate the properties of MARS and its feasibility to apply in wind turbines, an experiment should be designed and implemented to test the model wind turbine. Figure 5.1 shows an electric fan as the wind source. The fan is covered by plastic foils to avoid leakage of the wind from the fan. Figure 5.2 shows the output of the rotating wind turbine in the form of a lighted bulb. Figure 5.3 shows the measurement of the power output of the wind turbine by interfacing the bulb to an oscilloscope. The oscilloscope detects the wave pattern of the AC current generated

by the turbine. Figure 5.4 describes the evaluation of the performance of MARS. A bulb is connected to the generator.

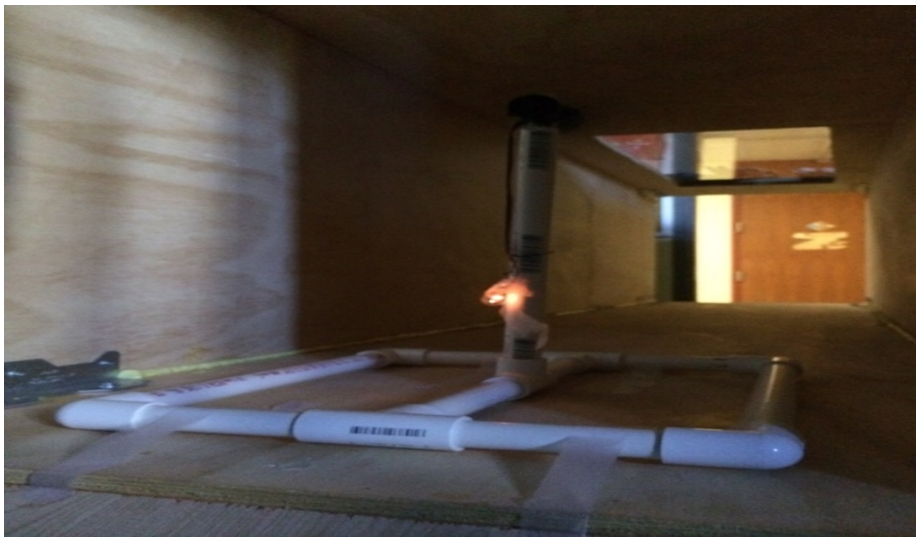

Figure 5.2 Electric current generated by rotating wind turbine passing through the bulb.

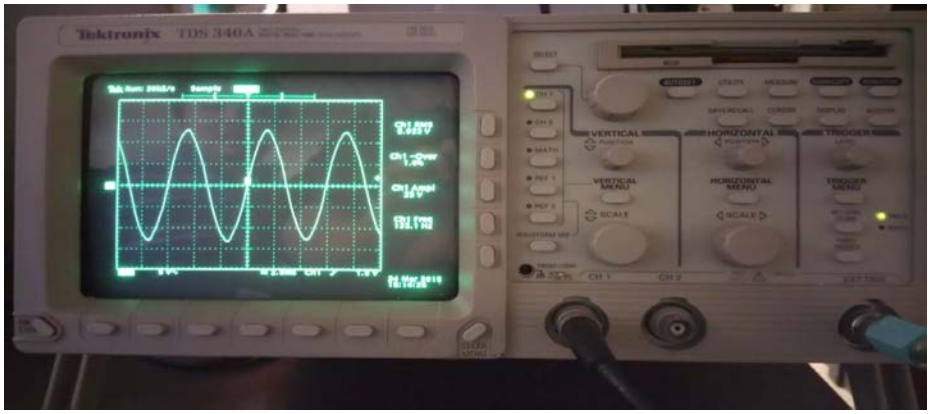

Figure 5.3 Rotating wind turbine linked to the bulb with the oscilloscope to collect the data of current produced by the turbine.

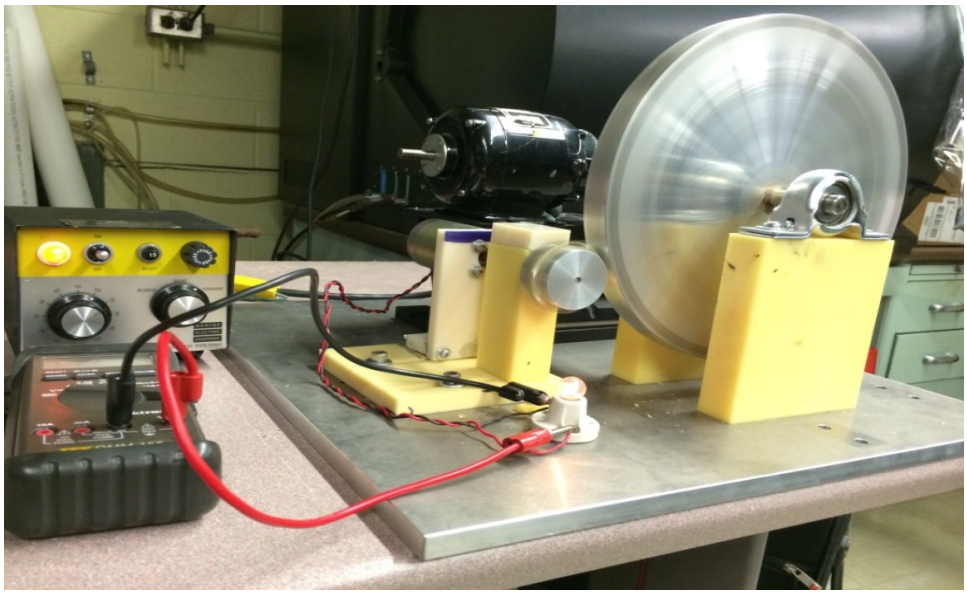

Figure 5.4 Rotating MARS with an electric motor as power source. The switch and the knob are used to control the motor. A multimeter is used to measure the voltage and the current in the bulb.

The diameter of the turbine swept area cannot exceed either the width or the height of the tunnel; thus, the size of the wind turbine is restricted. Table 5.1 shows the specifications of the wind tunnel. The most appropriate location for the test should have the least variance. This location is about 1 foot from the tunnel exit and half the height of the tunnel from the bottom. Table 5.2 shows the parameters of the wind turbine. Table 5.3 shows the test results of MARS.

Table 5.1 Wind Tunnel Parameters

Length	l	2.43m
Width	w	0.61m
Height	h	0.61m
Average Wind Velocity	v	4.6 m/s
Air Density	ρ	1.29 kg/m^3

Table 5.2 Parameters of the Wind Turbine

Swept Radius	R	0.2m
Number of Blades	B	4
Frequency of Blades	f	19Hz
Bulb Voltage	V	7.8V
Bulb Current	I	0.45A
Power Output of the Wind Turbine	P_t	3.51W
Power of the Wind	P_w	7.89W
Tip Speed Ratio	λ	0.826
Power Coefficient	C_p	44.5%

Table 5.3 Test Results of MARS

Angular Velocity of Driver Shaft	ω_0	467.5rpm
Angular Velocity of Driven Shaft	ω_1	1869rpm
Bulb Voltage	V	5.2V
Bulb Current	I	0.48A
Bulb Power	P_2	2.5W

5.2 Computer-Aided Engineering Software Simulation

5.2.1 Finite Element Analysis

Mathematically, the finite element analysis (FEA) is a numerical way to find the approximate solutions to boundary value problems for partial differential equations. The whole problem domain will be divided into smaller and simpler parts called finite elements. Then, by systematic recombination, subdomains with known equations will be formed into global system for ultimate calculations with given initial values. Connecting many simple equations applied to small subdomains, FEA could approach the best approximation over a larger domain by minimizing the associated error functions. Several advantages of this division are, for example, the accurate

representation of complicated geometry, inclusion of dissimilar material properties, the convenient representation of entire solution and collection of local effects. FEA is currently widely used in science and engineering to design, model, simulate new products that satisfy specific requirements before fabrication. It can also test or evaluate the performance of existing products by obtaining significant data prior to improvement or modification to new environment.

Two-dimensional (2-D) modeling and three-dimensional (3-D) modeling are the two modeling and analysis types used in FEA. Despite the simplicity and normal standard for computers to run 2-D modeling operation, 3-D modeling uses more complicated calculations and leads to more accurate results. There are numerous linear and non-linear functions for each modeling scenario. Linear functions are not as complicated as non-linear ones. For instance, the former does not consider plastic deformation of materials, but the latter does and it is applicable to the entire stage of a material until its rupture.

5.2.2 COMSOL Multiphysics Simulation

COMSOL Multiphysics is a general-purpose finite element analysis software package for physics and engineering applications, particularly for multiphysics or coupled phenomena. The software can be operated on multiple platforms such as Windows, Mac, Linux and it provides additional interfacing products that could associate the simulations with mainstream numerical tools and CAD software such as MATLAB and AutoCAD so that existing models created by these tools can be directly imported

to COMSOL that facilitate the modeling. With more than 30 add-on modules, the simulation could be expanded and researchers are able to further investigate in such dedicated physics interfaces. It also gives users the flexibility to define and customize their own partial differential equations and properties of materials.

Generally speaking, the main procedures of using COMSOL FEA software are including three sections: preprocessing, computation and postprocessing. Predefined parameters and variables of model and materials, model establishment, boundary condition settings and meshing are included in the preprocessing. Computation section includes choosing the partial differential equations, adjust solver settings. Postprocessing is used to obtain the desired visualization of results for certain variables and their dynamic change and tendency.

Multiphysics are always involved in real-life physical phenomena. Many physical simulations include coupled systems, for example, electromagnetic field is coupled by electric field and magnetic field. To increase the accuracy of simulation, appropriate tools that handle multiple physical models or multiple simultaneous physical phenomena are needed.

5.2.3 Modeling and Simulation Research

Figure 5.5 is the illustration of coaxial MARS model used in the simulation. The inner rotor is rotating clockwise at a constant angular velocity ω_i, the outer rotor is moving along the opposite direction at ω_o. Grey areas with arrows are permanent magnets and darker grey annular areas are the rotors made of soft iron. Purple areas are stationary

steel poles and white areas are air gaps. The steel poles and the air gaps are considered as magnetic field permeable materials. There are 5 pairs of magnetic poles in the outer rotor and 2 pairs of magnetic poles in the inner rotor. The alignment of magnet poles is circulated along peripheral direction periodically.

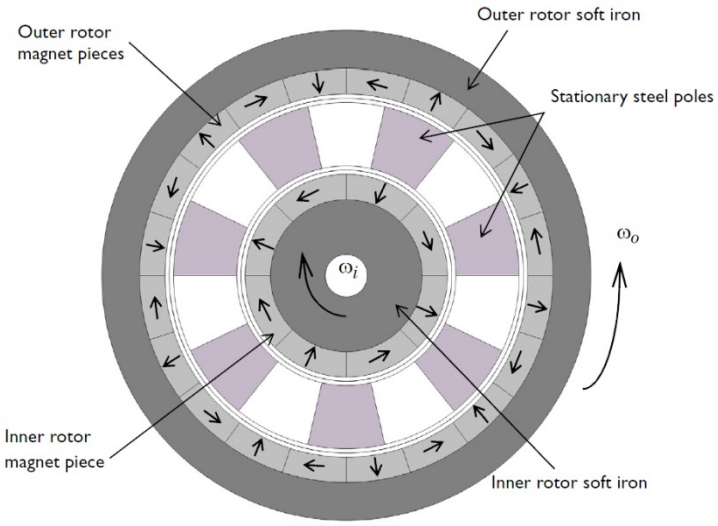

Figure 5.5 Model of coaxial MARS. The arrows indicate the direction of magnetization of magnets.
Source: http://www.comsol.com/model/magnetic-gear-in-2d-14583.

Figure 5.6 shows the magnetic flux density in a 2-dimensional plane. The force lines of magnetic field are connected from poles of magnets in the inner rotor to those in the outer rotor. When there is relative movement between the rotors, previous lines are disconnected and new lines are generated. The torque of the driver wheel will be transferred to the driven wheel by the interaction of magnetic lines of force.

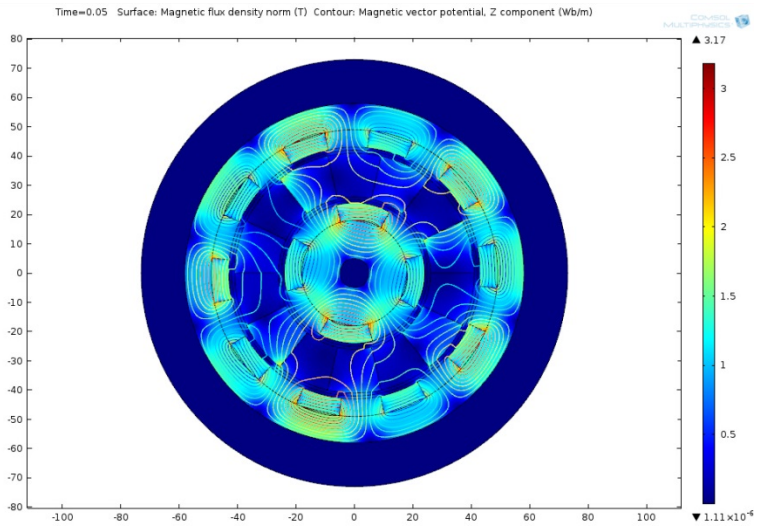

Figure 5.6 Magnetic flux density of coaxial MARS.

Actual tests are made to verify this proportional character and the above relation is indicated, as shown in Table 5.4. The ratio $\omega_1 : \omega_0$ is nearly equal to 4:1; it is revealed in the table as the "gear ratio" of MARS – it is the ratio of magnetic pairs of poles. MARS can work well similarly to the meshing of mechanical gears, controlling the transmission system.

Table 5.4 Relation of Angular Velocities between the Driver Wheel and the Driven Wheel with the Magnetic Poles Pairs Ratio 4:1

Driver Wheel ω_0	Driven Wheel ω_1	Ratio $\omega_1 : \omega_0$
8	30	3.750
60	245	4.083
120	470	3.917
180	700	3.889
240	950	3.958
467.5(Maximum)	1869	3.998

Figures 5.7 and 5.8 are graphs of axial torque values depending on time. An important relation found in these graphs is that the angular velocities in both rotors are doubled though the inner to outer speed ratio remains 5:2, which is equal to the

inverse ratio of corresponding magnetic poles pairs. From Figures 5.7 and 5.8, it is observed that when the axial torque of inner rotor is at its peak, the axial torque of the outer rotor is at its valley (for example, at about 0.0025s). When the rotors keep moving, the torque will be transferred, and the axial torque of the inner rotor will decrease to its valley while the outer rotor axial torque will be at its maximum. This process is called magnetic coupling. The magnetic poles are just like the teeth of mechanical gears, meshing and transmitting mechanical power.

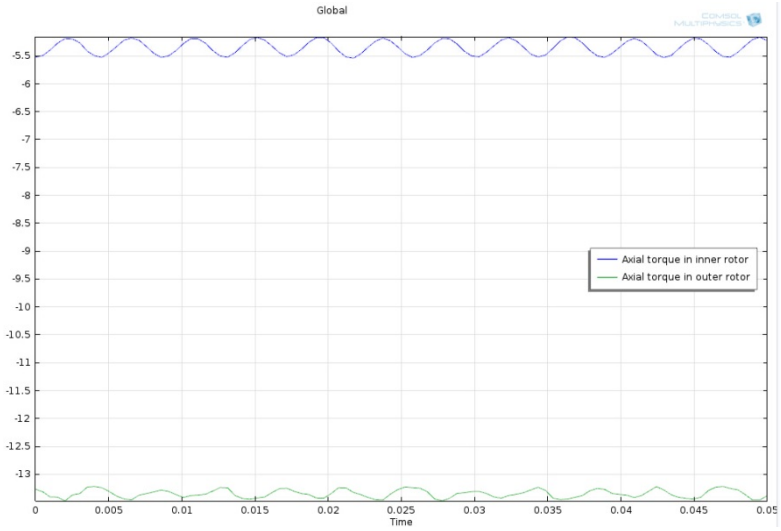

Figure 5.7 Axial torque of outer and inner rotor when outer rotor RPM is 200 and inner rotor RPM is 500.

Magnetic coupling is a means of transferring torque from one shaft to another without a physical mechanical connection. Magnetic shaft couplings are most often used for liquid pumps and propeller systems, since the two shafts can be separated and sealed to avoid exposure of inside fluid to air, thus taking place of shaft seals that suffer wear and failure.

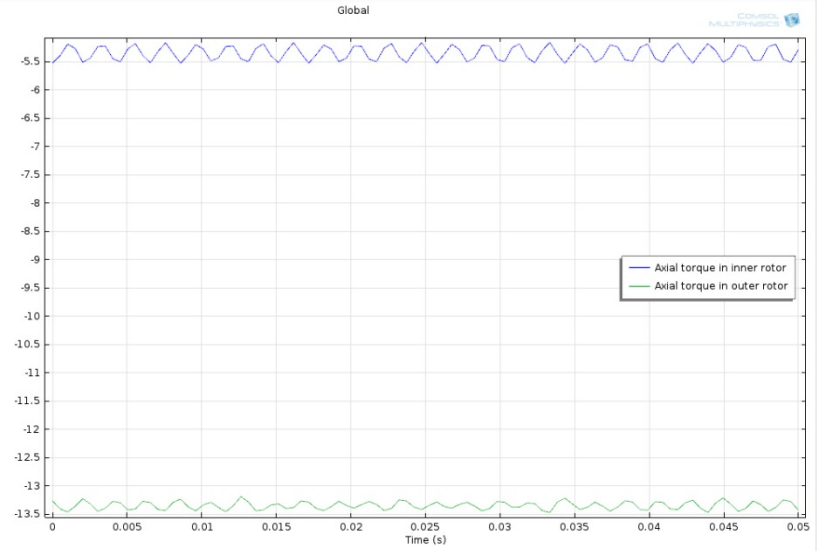

Figure 5.8 Axial torque of outer and inner rotor when outer rotor RPM is 400 and inner rotor RPM is 1000.

CHAPTER 6

CONCLUSIONS

The wind turbine performs well in wind tunnel experiments and its aerodynamic properties such as power coefficient and tip speed ratio is within reasonable range. The “gear ratio” of MARS is always proportional to the number of magnetic poles. The magnetic coupling transfers torque well though with a little lag and ripple.

There are still drawbacks in the entire project. First, the scale of the wind turbine and wind tunnel could be larger if condition allowed. The output power of wind turbine is small to replace the electric motor as the prime mover. Therefore, MARS and the turbine could not be integrated and experimented as a whole. Second, the measurements of essential variables and parameters are still not precise enough; this may influence the accuracy of test results. Third, proper model of MARS is complicated to establish in computer software simulation, thus preventing current theoretical simulation from being closer to the real condition.

MARS offers a very promising approach to power generation for low power needs such as solid state lighting, wheel chairs, electric vehicles etc. Contactless gears have the potential to replace mechanical gears in the very near future.

REFERENCES

[1] Russo U, Capolongo F (1990) An Outline of the Prehistory of Magnetism. In: Long GJ, Grandjean F (eds) Supermagnets, Hard Magnetic Materials. Kluwer Academic Publishers, Dordrecht, Netherlands, pp 7-26.

[2] Lane, FC (1963) The Economic Meaning of the Invention of the Compass, Am Hist Rev 68: 605-617.

[3] Herny, J (2001) Animism and Empiricism: Copernican Physics and the Origins of William Gilbert's Experimental Method, J Hist Ideas 62: 99-119.

[4] Kouveliotou C, Duncan RC, Thompson C (2003) Magnetars, Sci Am 288: 34-41.

[5] Milton, KA (2006) Theoretical and Experimental Status of Magnetic Monopoles, Rep Prog Phys 69: 1637-1711.

[6] Goddard P, Olive DI (1977) New Developments in the Theory of Magnetic Monopoles, Rept Prog Phys 41: 1357.

[7] Jackson, JD (1999) Classical Electrodynamics 3rd edn. John Wiley & Sons, New York, NY, USA, p 186.

[8] Chikazumi, S (2009) Physics of Ferromagnetism 2nd edn. Oxford University Press, Oxford, UK, p 118.

[9] Halliday D, Resnick R (1970) Fundamentals of Physics. John Wiley & Sons, New York, NY, USA, pp 452-453.

[10] Serway, RA (1996) Physics for Scientists and Engineers with Modern Physics 4th edn. Saunders College Pub, Philadelphia, PA, USA, p 687.

[11] Chow, TL (2006) Electromagnetic Theory: A Modern Perspective. Jones and Bartlett, Sudbury, MA, USA, p 134.

[12] Merzouki R, Samantaray AK, Pathak PM, Ould Bouamama B (2012) Intelligent Mechatronic Systems: Modeling, Control and Diagnosis. Springer, London, UK, pp 403-405.

[13] Voit W, Kim DK, Zapka W, Muhammed M, Rao KV (2001) Magnetic behavior of Coated Superparamagnetic Iron Oxide Nanoparticles in Ferrofluids. MRS Online Proceedings Library 676. doi:10.1557/PROC-676-Y7.8.

[14] Planck, M (1923/1927) in Ogg, A (trans) Treatise on Thermodynamics 3rd edn. Longmans, Green & Co, London, UK, p 40.

[15] Neuland, AH (1916) Apparatus for Transmitting Power. US Patent 1171351 A.

[16] Faus, HT (1941) Magnet Gearing. US Patent 2243555 A.

[17] Fraden, J (2010) Handbook of Modern Sensors: Physics, Designs, and Applications 4th edn. Springer, New York, NY, USA, p 73.

[18] Abdel-Khalik AS, Ahmed S, Massoud A (2014) Alexandria Engineering Journal 53: 573-582.

[19] Hatch, GP (2010) A Bearingless Coaxial Magnetic Gearbox. Magnetics 2010 Conference, Lake Buena Vista, Florida, USA.

[20] Li X, Chau K-T, Cheng M, Hua W (2013) Comparison of Magnetic-Geared Permanent-Magnet Machines, Progress in Electromagnetics Research 133: 177-198.

[21] Ravindra, NM (2015) Intelligent Manipulation of Controllable Magnetic Fields – Concept to Realization. The International Conference on Materials Science SCI Indexing (ICMS 2015), Shanghai, China.

[22] Gipe, P (1993) The Wind Industry's Experience with Aesthetic Criticism, Leonardo 26: 243-248.

[23] Barthelmie RJ, Pryor SF, Tronæs S et al (2010) Quantifying the Impact of Wind Turbine Wakes on Power Output at OffshoreWind Farms, J Atmos Ocean Tech 27: 1302-1317.

[24] Akhmatov V, Knudsen H (2002) An Aggregate Model of a Grid-Connected, Large-Scale, Offshore Wind Farm for Power Stability Investigations-Importance of Windmill Mechanical System, Int J Elec Power 24: 709-717.

[25] Toonen HM, Lindeboom HJ (2015) Dark Green Electricity Comes from the Sea: Capitalizing on Ecologicalmerits of Offshore Wind Power?, Renew Sust Energ Rev 42: 1023-1033.

[26] Eriksson S, Bernhoff H, Leijon M (2008) Evaluation of Different Turbine Concepts for Wind Power, Renew Sust Energ Rev 12: 1419-1434.

[27] Berglund B, Lindvall T, Schwela DH (1999) Guidelines for Community Noise World Health Organization (WHO), Geneva, Switzerland.

[28] Shaltout ML, Yan Z, Dushyant Palejiya, Chen D (2015) Tradeoff Analysis of Energy Harvesting and Noise Emission for Distributed Wind Turbines, Sustainable Energy Technologies and Assessments 10: 12-21.

[29] Prabhakarana S, Krishnarajb V, Senthil Kumarb M, Zitoune R (2014) Sound and Vibration Damping Properties of Flax Fiber Reinforced Composites, Procedia Engineering 97: 573-581.

[30] Alexandrova Y, Semken RS, Pyrhönen J (2014) Permanent Magnet Synchronous Generator Design Solution for Large Direct-Drive Wind Turbines: Thermal Behavior of the LC DD-PMSG, Appl Therm Eng 65: 554-563.

[31] Greco A, Sheng S, Keller J, Erdemir A (2013) Material Wear and Fatigue in Wind Turbine Systems, Wear 302: 1583-1591.

[32] Dalili N, Edrisy A, Carriveau R (2009) A Review of Surface Engineering Issues Critical to Wind Turbine Performance, Renew Sust Energ Rev 13: 428-438.

[33] Maissan, JF (Mar. 2001) Wind Power Development in Sub-Arctic Conditions with Severe Rime Icing. Circumpolar Climate Change Summit and Exposition, Whitehorse, Yukon, Canada.

[34] Bavanish B, Thyagarajan K (2013) Optimization of Power Coefficient on a Horizontal Axis Wind Turbine Using Bem Theory, Renew Sust Energ Rev 26: 169-182.

[35] Ragheb M, Ragheb AM (2011) Wind Turbines Theory - The Betz Equation and Optimal Rotor Tip Speed Ratio. In: Carriveau R (ed) Fundamental and Advanced Topics in Wind Power, InTech, Rijeka, Croatia.

[36] Department of Mechanical Engineering at Boston University, Lift and Drag, http://people.bu.edu/dew11/liftanddrag.html. Accessed 04/18/2015.

[37] Johnson KE, Pao LY, Balas MJ, Fingersh LJ (2006) Control of Variable-Speed Wind Turbines: Standard and Adaptive Techniques for Maximizing Energy Capture, IEEE Contr Syst Mag 26: 70-81.

[38] Heier, S (2005) Grid Integration of Wind Energy Conversion Systems. John Wiley & Sons, Chichester, UK, p 45.

[39] Kaltschmitt M, Streicher W, Wiese A (2007) Renewable Energy: Technology, Economics and Environment. Springer Science & Business Media, New York, NY, USA, p 55.

[40] The 10 Biggest Turbines in the World. http://www.windpowermonthly.com/10-biggest-turbines, Accessed 04/19/2015.

[41] Manwell JF, McGowan JG, Rogers AL (2010) Wind Energy Explained: Theory, Design and Application. John Wiley & Sons, New York, NY, USA.

[42] Nagai BM, Ameku K, Roy JN (2009) Performance of a 3 kW Wind Turbine Generator with Variable Pitch Control System, Appl Energ 86: 1774-1782.